J. Condensed Matter Nucl. Sci. 34 (2021) 1–31

Research Article

A Review of Negative LENR Experiments, Determining Why They Failed, and How They Impacted the Field

P.A. Mosier-Boss* and L.P. Forsley
GEC, 5101B Backlick Rd., Annandale, VA 22003

M.H. Miles
College of Science and Technology, Dixie State University, St. George, UT 84790

Abstract

On March 23, 1989, Fleischmann and Pons made the sensational claim that they had achieved nuclear fusion electrochemically using Pd cathodes in LiOD/D_2O electrolytes. Despite reservations, scientists worldwide went into their laboratories attempting to replicate the Fleischmann–Pons discovery. There were some successes but a greater number of failures. A preponderance of those negative reports came from prestigious institutions, which caused a majority of members in the scientific community to dismiss the LENR field. In this communication, we re-examine some of the most noteworthy negative experiments, discuss why they failed, and how they impacted the field.
 ISSN 2227-3123

Keywords: Replications, Electrolysis, Gas Phase, Heat, Nuclear Ash

1. Introduction

On March 23, 1989, at the University of Utah, Martin Fleischmann and Stanley Pons [1] held a press conference where they announced that they had "established a sustained nuclear fusion reaction by means that are considerably simpler than conventional techniques." Then, holding a cell as a prop, Pons briefly described the experiment that drove deuterons inside the lattice of a palladium rod to such an extent that fusion of the deuterons occurred with a considerable release of energy. It should be noted that Fleischmann and Pons had never used this cell in any of their actual experiments. Fleischmann further indicated that the cells they used were Dewar flasks that allowed them to accurately measure the heat that was produced. The press conference was an unorthodox means of announcing an important scientific discovery, although a preliminary paper on their results had already been accepted in a journal. However, there were extenuating circumstances involving another university which prompted the University of Utah to announce the discovery via a press conference rather than going through the accepted journal process and peer review.

*Corresponding author: pboss@san.rr.com; (858) 576-6415

 ISSN 2227-3123

The events leading up to the press conference have been documented in great detail in other books and will not be discussed here [2-4].

Initially, Fleischmann and Pons only had calorimetry measurements that showed that more heat was produced than could be accounted for by chemical means. From this they concluded that the excess heat had to be nuclear in origin. Their intent had been to announce their discovery after ~18 months of additional experiments to look for nuclear ash, such as gamma rays, neutrons, and tritium. However, a few weeks prior to the announcement, they quickly conducted additional experiments looking for evidence of this nuclear ash. Again the reason for this urgency has been documented in other books [2-4] and will not be discussed here. On March 13, 1989 [5], ten days prior to the press conference, Fleischmann and Pons submitted a hastily written paper [6] to the Journal of Electroanalytical Chemistry (JEAC). The paper was quickly reviewed, was accepted on March 22, 1989 (one day prior to the press conference), and was published on April 10, 1989. Later, Fleischmann told Miles that he never would have agreed to the press conference if their first cold fusion manuscript had not been already accepted by Roger Parsons, who was then Editor of JEAC. Preprints of the paper were leaked out prior to its publication and it was rapidly disseminated among the scientific community. However, in 1989, there was no Internet or e-mail. The only method available to quickly distribute information was by fax machine and, by the time someone got a fax of a fax of a fax, it was pretty faded but, none-the-less, you were happy to get it. Unfortunately, the publication was disappointing as it provided no details on how the cells were constructed, the charging protocol used, the type of calorimeter used and data analysis, *etc*.

The announcement by Fleischmann and Pons did create quite a sensation and excitement. Pons and Fleischmann made headlines in newspapers and were featured on the covers of magazines. The news media referred to the Fleischmann–Pons discovery as "cold fusion" and the moniker stuck. The response by the scientific community to the Fleischmann–Pons announcement was likewise instantaneous but, in general, was not as enthusiastic or positive. The community noted that, at the time of the announcement, there weren't any refereed papers. Also the experiments had neither been replicated nor were they repeatable, and that the experimental results did not match theory. How could eV chemical reactions initiate MeV (1,000,000 eV) products? Also, if the reaction was nuclear in origin, where were the neutrons? Despite these questions, scientists worldwide went into their laboratories in attempts to replicate the Fleischmann–Pons discovery. They used palladium whose history had not been known. They built cells that resembled the prop used by Fleishmann and Pons during their press conference. Cells of this design displayed poor mixing. Experiments that were done depended upon what resources were available in the laboratories as well as the expertise of the scientists themselves. Some researchers did electrolysis and calorimetry. Gas loading of palladium was pursued by other scientists. Rather than doing calorimetry, others focused on looking for nuclear ash. There were some successes but a greater number of failures. It was easier to publish negative results than it was to publish positive ones. This preponderance of negative reports, some from highly reputable institutions, such at Caltech, MIT, Harwell (U.K.), and UC Berkeley, caused the scientific community to dismiss the LENR field. Yet many of the experiments yielding negative results were flawed. Part of the problem was due to the fact that, in the early days, not much was known about the phenomenon. As a result, improper/inadequate instrumentation and experimental designs were employed. This was not understood until much later but the damage to the field had been done. In other rare cases, there are indications of scientific maleficence. In this review, we focus on some of the most noteworthy negative experiments and discuss why they failed and how they impacted the field.

2. Calorimetry and Helium-4

2.1. Summary of Fleischmann–Pons Cells and Calorimeter

Figure 1a shows a schematic of the electrochemical cell used by Fleischmann and Pons in their calorimetry [7]. They used a Dewar-type isoperibolic calorimeter to measure the heat produced during electrolysis. Advantages of this

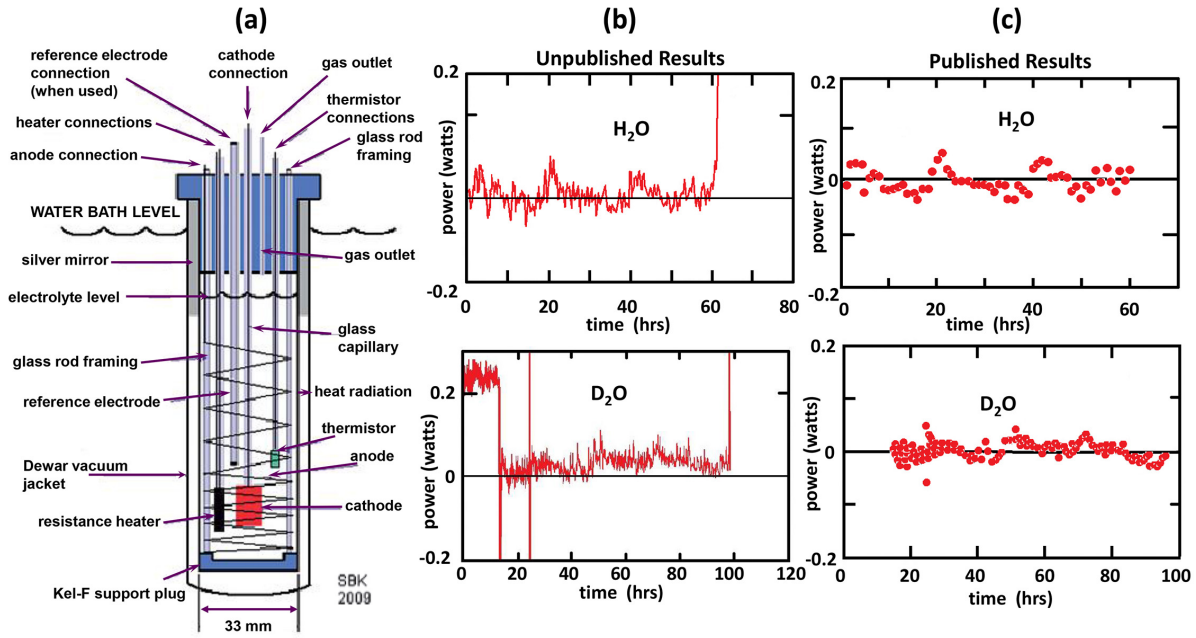

Figure 1. (a) Schematic of a Fleischmann–Pons electrolytic cell (not to scale). The Pt anode wire was wound in a helical configuration around glass support rods, surrounding, with a fairly even distribution, the Pd cathode in the center [7]. Reprinted with permission from Steve Krivit. MIT excess power data where (b) and (c) show the unpublished and published results, respectively [14].

approach include a wide dynamic range for both the cell temperature and cell input power, direct visual observations inside the cell during calorimetric experiments, relative low cost, self-purification of the system, the safety of an open system, and heat transfer mainly by electromagnetic radiation [8, 9]. The use of control or "blank" experiments, such as replacing palladium by platinum, show that anomalous excess power is measurable to within ±0.1 mW (± 0.01% error) using this electrochemical calorimetry. The temperature error was ± 0.001K, which was achieved using calibrated thermistors. This accuracy requires the use of seven power terms to adequately describe the rate of enthalpy flowing into and out of the calorimetric system where Eq. (1) is the complete expression for isoperibolic calorimetry:

$$P_{calor} = P_{EI} + P_X + P_H + P_C + P_R + P_{gas} + P_W. \quad (1)$$

The net power that flows into and out of the calorimetric system (P_{calor}) is determined by the electrochemical power (P_{EI}), excess power (P_X), the internal heater power (P_H), the heat conduction power (P_C), the heat radiation power (P_R), the power carried away by the gases generated (P_{gas}), and the power due to pressure–volume work (P_W). It should be noted that Fleischmann and Pons did not use P_W term in their data analysis. Miles added the P_W term some years later when he was doing calorimetry at NHE using the Pd-B alloy. He found that the P_W term became important at high cell currents. Each power term in Eq. (1) is a function of time (t), such as $P_{calor} = C_p M \mathrm{d}T/\mathrm{d}t$, where C_p is the heat capacity of D_2O, M is the mass of the calorimetric system, and T is temperature. Thus Eq. (1) is a differential equation that can be used directly or numerically integrated for greater accuracy.

The glass Dewar cells designed by Fleischmann and Pons in 1993 were 25 cm in height and narrow (2.5 or 3.30 cm I.D.) so that the bubbling action of D_2 and O_2 emerging from the surface of the anode and cathode served to keep the electrolyte well mixed. Fleischmann and Pons used two methods to demonstrate that the fluid in their cells were

well mixed [10]. They used video to measure the time it took for a drop of red dye to be homogeneously mixed in the electrolyte. For the lowest electrolysis power level used in their experiments, it took the bubbles from electrolysis 3 s horizontally and 20 s vertically to disperse the red dye into the electrolyte. Faster mixing occurred for higher input powers. An array of five thermistors arranged vertically and horizontally through the cell showed that the temperature variations in the liquid were at most 0.005°C (except at the bottom of the cell where they were 0.01°C). There was a high vacuum between the inner and outer glass surfaces of the cell. The double wall of the Dewar vacuum flask prevented heat conduction out of the sides and bottom of the cell. Heat flow out of the cell would be by means of radiant emission to the bath water. However, with time the vacuum inside these Dewar vacuum flasks will slowly fail. When newly constructed (and depending upon the skill of the glass blower), heat transfer due to conduction would be about 2%–3%. The Dewar's vacuum insulation and effervescent bubbling action from anode and cathode kept the temperature of electrolyte sufficiently uniform to permit accurate heat flow measurement. After ICCF2 in Como, Italy, the cells were silvered. This silver coating, which was inside near the top and down to below the level of the electrolyte, limited heat loss through the top and made the heat loss value less dependent on the changing liquid level. With this design 95% of the heat was removed by radiation and 5% by conduction. There was a calibration heater used to apply heat pulses to calibrate and monitor the rate of radiant heat transmission by the cell to the surrounding water bath. The cells were operated in a constant current mode. The open cells were self-purifying. Ordinary H_2O acts as a poison in the Fleischmann–Pons effect (FPE). In an open cell, H is preferentially electrolyzed versus D at the cathode. Consequently, any H_2O contamination will be gradually removed during electrolysis. In closed systems, the initial H_2O contamination will remain trapped throughout the experiment.

It should be noted that Fleischman and Pons had perfected their isoperibolic Dewar calorimetry over at least five years prior to their 1989 announcement [9]. This included determination of the optimum size and shape of their calorimetric cell, attaining a good Dewar vacuum, improving their temperature measurements, acquiring good instrumentation, setting up a reliable data acquisition system, modeling their calorimetry with correct equations, and improving their methods for the analysis of the calorimetric data. Recently Miles [11] indicated that when Fleischmann and Pons started their research, they did not know how large the effect, if any, there would be. Therefore, they wanted the calorimetry to be as accurate as possible where even 1.0 mW of excess power could be detected. They realized that if nuclear reactions inside the Pd lattice were similar to hot fusion, then even 1.0 mW of excess power would have produced about 10^8 neutrons per second, which would have been an unsafe amount. It is not surprising, given the limited time after the 1989 announcement, that others did not achieve the same level of accuracy as that of Fleischmann and Pons which, in turn, often resulted in negative results.

2.2. Caltech (U.S.)

A variation of isoperibolic calorimetry was done at the California Institute of Technology, Caltech [8]. While they had a Tronac Model 1250 vacuum-jacketed calorimetric Dewar, most of the reported results were for an air-jacketed "Dewar" that contained 30 mL of electrolyte. Lewis of Caltech referred to their calorimeter cell as a "Dewar." However a Dewar flask is another name for a vacuum flask and a vacuum flask cannot be air filled. Because the Caltech "Dewar" walls contained 1 atm of air, there was no vacuum and heat conduction, not electromagnetic radiation, was the main heat transfer pathway. A schematic of the calorimeter in a later Caltech publication showed that the cell was short and fat with a length/diameter ratio of only 1.4 versus a ratio of 10 (25 cm/2.5 cm) for the Fleischmann–Pons cells used at the NHE laboratory in Sapporo, Japan, around 1993. Because the Caltech cell was short and fat, stirring was required to keep the electrolyte homogeneously mixed. A motor was used to vigorously stir the electrolyte. The Joule heating resulting from stirring (∼0.3°C) had to be accounted for in all measurements. Caltech measured temperatures to within ±0.03K and the calorimetric error was ± 3 mW [12]. Only fragments of Eq. (1), P_{EI} and a term for total power similar to P_C, were used to analyze the data [8]. Also the cell constant was allowed to arbitrarily change with

time in the Pd/D_2O experiment [13]. Changing the cell constant would effectively zero out any excess power. No such changes in the cell constant occurred in their Pd/H_2O experiment and both the H_2O and D_2O experiments used the same glassware and other components in the same configuration. This suggests that the temperature increase observed by Caltech was real and was caused by anomalous heat.

Caltech submitted their findings to *Nature* less than two months after the initial announcement of the FPE [8]. A single Fleischmann–Pons experiment using bulk Pd generally requires 4–8 weeks of electrolysis so it is unlikely that they achieved the conditions to initiate the effect. Caltech reported no evidence of excess enthalpy, neutron, gamma ray, tritium, or helium production during electrolysis.

2.3. Harwell (U.K.)

Harwell laboratory in the U.K. hastily performed experiments in 1989 [8]. The Fleishmann-Pons type Dewar calorimeter used by Harwell had an inner diameter of 2.5 cm, a height of 10 cm, no silvering, and had an error of 15%. Given the dimensions of the cell, stirring by the electrolysis gases would be adequate. A single thermistor was used that was positioned in the upper half of the cell. The Dewar had a poor vacuum. The Harwell isoperibolic calorimetry shows only the use of the P_{EI} term and approximations for P_{gas}, P_R, and P_C [12]. Harwell measured temperatures to within $\pm$0.1K and the calorimetric error was $\pm$ 10 mW [12]. Other error sources include their method of cell calibration and the unfavorable geometry of various cathodes (beads, ribbon, bar) used [8]. These unfavorable cathode geometries would not provide for uniform electric fields and symmetry required for high deuterium loadings. Independent analysis of the Harwell data indicated that their cells were unlikely to produce significant excess heat because of low current densities, low levels of D loading into the Pd, as well as these poor choices in their experimental design.

2.4. MIT (U.S.) and Scientific Misconduct

MIT, in Cambridge, MA, stated that no excess output power or any other evidence of fusion products (neutrons, gamma, helium, and tritium) was detected [8]. Dewar cells were not used, thus the main heat transfer pathway was by conduction rather than by electromagnetic radiation as in the Fleischmann–Pons Dewar cells. The Phase I calorimetry was admittedly relatively crude with error limits of $\pm$0.3 W. The two Phase II calorimeters were greatly improved and consisted of reasonable cell dimensions of 12 cm in height and a narrow 2.1 cm in diameter. Unlike the short, fat cells used by Caltech, no mechanical cell stirring was necessary. MIT calorimeters used a large excess of glass wool thermal insulation in the compartment between the cell and water bath. As a result the desired heat flow pathway from the cell to the constant temperature bath was severely blocked. The major heat transfer pathway was out of the cell top to the room temperature air. The Pt resistance temperature detector (RTD) thermometer used in each cell by MIT had an accuracy of $\pm$ 0.1 K compared to $\pm$0.001 K for the two thermistors used in each Fleischmann–Pons Dewar cell. The sensitivity of the Phase II MIT calorimeters was stated at $\pm$40 mW contrasted to $\pm$0.1 mW sensitivity for the F-P Dewar calorimeters. The MIT isoperibolic calorimetry used terms corresponding to P_{EI} , P_H, and P_C . From the dimensions of the MIT Pd rod cathodes (0.1 cm $\times$ 9 cm), the expected excess power of about 70 mW would not be easily distinguished from the $\pm$40 mW calorimetric error. MIT reported their key calorimetric measurements over a rather short time period (100 h). The observation of measurable excess power with Pd cathodes in D_2O generally requires 6 days or more of electrolysis.

It has been claimed that there was a serious discrepancy between the unpublished raw data and the final published data for the MIT D_2O cell [8, 14]. This is illustrated in Figure 1b [14]. In the plot of the unpublished data there is a clear evidence of excess heat (beyond electrical input power) in the D_2O cell, but no visually apparent excess in the H_2O cell. The results that were published in the *Journal of Fusion Energy* shows no excess heat for D_2O. The D_2O data points appear to be arbitrarily shifted down to make the apparent excess power vanish. Extensive analysis performed by Dr.

Mitchell R. Swartz concluded that the MIT H_2O and D_2O data sets were "asymmetrically" treated. This controversy caused MIT to change their calorimetric conclusion from the previous "failure-to-reproduce" to "too-insensitive-to-confirm". It should be noted that the D_2O cell showed an increasing cell temperature and a corresponding decreasing cell voltage that was not present in the H_2O cell. When cells are operated at a constant current, a decrease in cell voltage is indicative of heat production.

2.5. Earthtech (U.S.) and MOAC

At NHE, Miles [15, 16] used the Fleischmann–Pons Dewar type cells to investigate the Pd–Ce–B, Pd–B, and Pd–Ce cells. Significant excess power was produced from the cells using the Pd–B and Pd–Ce alloy cathodes. In contrast, the Pd–Ce–B alloy showed no measurable excess power. The same Pd–Ce cathode that was used at NHE produced significant excess power in earlier experiments at China Lake. Previous experiments at China Lake using similar Pd–B alloy cathodes produced excess heat in seven out of eight experiments [17]. The Pd–B alloy cathode that failed had a large, folded-over metal region that acted as a long crack and the cathode was poorly aligned in the cell. Both the folded region and poor alignment would result in low loading of deuterium in the cathode. For Pd–B cathodes that produced heat, it was shown that excess power could be obtained in repeated experiments using the same cathode.

EarthTech (Austin, TX) had developed a mass flow calorimeter with an accuracy of 0.1% [18]. They called the calorimeter MOAC (Mother Of All Calorimeters). They claimed that MOAC was quite reliable. The largest source of error was the drift exhibited by the thermistors used for the critical inlet and outlet water temperature measurements. They said that the observed drift was usually quite slow and was only a fraction of the manufacturer's specification meaning that the thermistors were performing significantly better that the manufacturer's guarantee. Because of this drift, MOAC required recalibration once every month or two.

In 2004, Miles spent a weekend at the EarthTech laboratory setting up a Pd-B experiment in their MOAC calorimeter. Due to rain, the humidity was high. They had no means of keeping moisture out while setting up the experiment. There was a problem with welding the wire lead to the Pd-B cathode. The D_2O cell had to sit some 30 min exposed to the high humidity atmosphere while this problem was solved. Miles was able to monitor the calorimetric results remotely on his computer back at the University of La Verne. There were numerous times Miles thought that there was excess power. Every time a small excess power effect was reported to EarthTech, the system would be recalibrated which would change the cell constant and zero out any heat effects. This was very similar to what Caltech did, as was discussed *vide supra*.

2.6. Helium-4 Measurements

2.6.1. *Naval Air Warfare Center China Lake (U.S.)*

In 1990, Miles *et al*. [19, 20] showed that excess heat correlated temporally with the production of ^{4}He. In these experiments, the gases evolved during electrolysis were collected and were sent away for analysis using a high resolution mass spectrometer. Figure 2a shows a schematic of their apparatus used to collect samples of effluent gas [19]. All connecting lines, as well as the cell, were flushed vigorously with boil-off nitrogen, which contained no ^{4}He, for at least 10 min prior to attaching a gas collection flask. The collection flasks were connected to the cell for at least two days of D_2O electrolysis before removal. Figure 2b is a schematic of the activated cryofiltration system used to remove all gases except helium. Nine samples were collected and analyzed. Figure 2c summarizes the calorimetric results of two identical isoperibolic calorimetric cells that were run in series (cells A and B each with two thermistors) in a constant temperature bath set at 27.50°C [20]. Sample collections are indicated and the results are summarized in the table in Figure 2d. The mass spectrometer was operated at its highest sensitivity. The instrument had sufficient resolution to baseline separate D_2 and ^{4}He. The detection limit for ^{4}He was determined to be 0.1 ppb, or 2×10^{12}

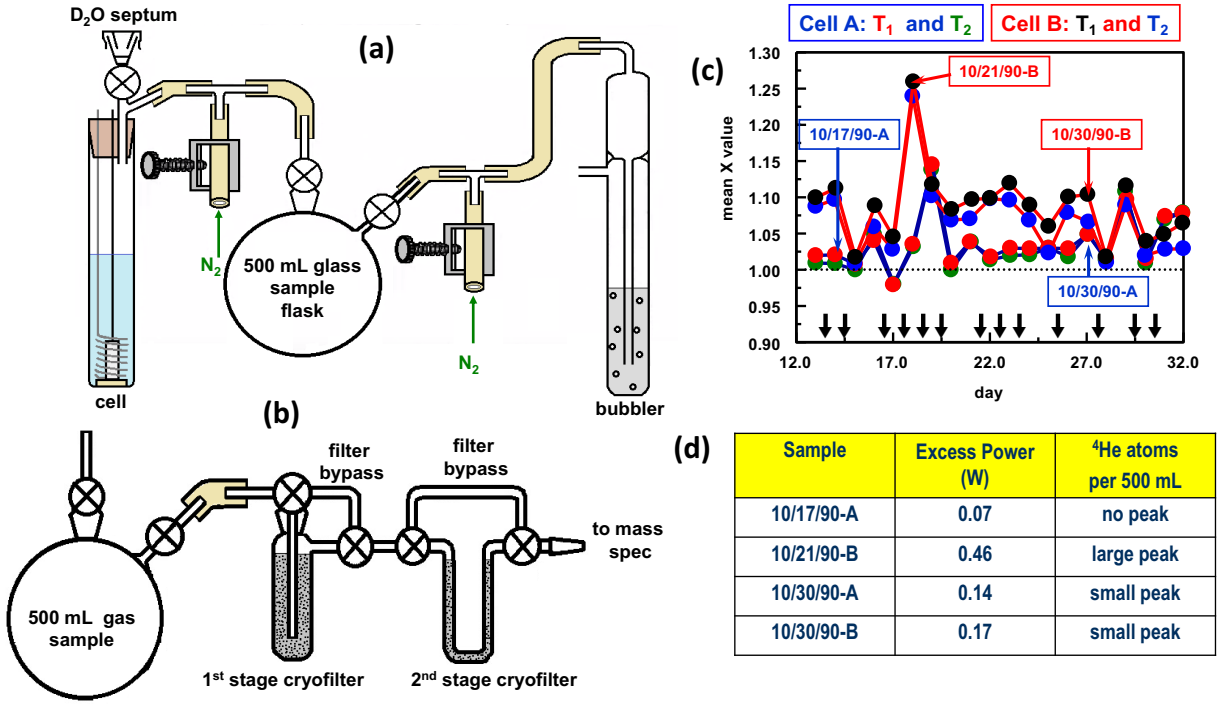

Sample	Excess Power (W)	^{4}He atoms per 500 mL
10/17/90-A	0.07	no peak
10/21/90-B	0.46	large peak
10/30/90-A	0.14	small peak
10/30/90-B	0.17	small peak

Figure 2. (a) Schematic of electrolytic cell with positive pressure gas discharge line used to collect samples of effluent gas [19]. (b) Schematic of the two stage activated cryofilter designed to remove all gases except helium [19]. (c) Calorimetric measurements and effluent gas collection dates in D_2O + LiOD for cell A (red and green filled circles) and cell B (black and blue filled circles) [20]. Electrolyte was 0.2 M LiOD in D_2O. Current density was 200 mA cm^{-2}. The symbol, down arrow, indicates when D_2O was added. (d) Helium and heat production during D_2O electrolysis [20].

^{4}He atoms in 500 mL of nitrogen. As can be seen for the results summarized in Figures 2c and d, ^{4}He was observed in those samples collected when the cell was producing excess heat. Furthermore the magnitude of the ^{4}He signal directly correlated with the amount of heat produced. No ^{3}He was detected in any of the samples. Neither ^{4}He nor ^{3}He were detected in the effluent gas when the electrolyte was replaced with LiOH in H_2O [19].

2.6.2. *Caltech (U.S.)*

Caltech [8] had also made attempts to measure helium in the effluent gas. They indicated that they had not detected any helium. However, the detection limit of their measurements was 1 ppm or 1000 ppb. Miles calculated that, to reach 1000 ppb ^{4}He in the electrolysis gas, the excess power would have to be about 10 W. Most calorimetric cells would boil with 10 W of input power.

3. GAS LOADING

3.1. SRI (U.S.)

At ICCF-7 Case [21] reported on D_2/H_2 gas loading of Pd on activated carbon catalyst. He claimed an excess temperature effect where temperature differentials between D_2 and H_2 of greater than 20 °C were measured. Gas samples were

sent to Oak Ridge National Laboratory (ORNL) where they measured 100 ppm ^{4}He in D_2. SRI did a replication of this experiment [22]. Separate stainless steel reaction vessels, containing identical amounts of catalyst from the same batch, were used. One vessel was used only for H_2 loading while the other was used solely for D_2 loading. During the experiments periodic measurements of ^{4}He were made by direct connection to a mass spectrometer capable of resolving the mass-4 peaks of D_2 and ^{4}He. In these experiments, heat was measured with D_2 loading but not H_2. All cells operated with H_2 showed no increase in ^{4}He over long periods of time. Some D_2 cells exhibited a slow, approximately exponential increase in ^{4}He with time. Other D_2 cells displayed no measurable increase in ^{4}He for a period of several days followed by a rapid approximately linear rise in ^{4}He to levels sometimes exceeding that of the ambient background.

3.2. Naval Research Laboratory (U.S.)

The experimental approach used by SRI significantly differed from that used by NRL in their gas loading experiments using either Pd on zeolite [23] or zirconium–nickel–palladium alloys [24]. In their experiments, NRL used a single reaction vessel loaded with either Pd on zeolite or Zr–Ni–Pd alloy. They would then alternate loading the sample with H_2 and then D_2. For Pd on zeolite they observed that Pd particles $<$ 2nm in size produced heat when D_2 was used and not H_2 [23]. They said that, in some zeolite matrices, the likely source of the heat was D-H exchange but not true of others. In fact, their experimental approach using a single reaction vessel and alternating D_2/H_2 loading accentuated D-H exchange. This is not the case of the SRI gas loading experiments which used two reaction vessels where one was dedicated to D_2 loading and the other H_2 loading. In the Pd on zeolite experiments, NRL indicated that weak X-rays and intense light emissions were observed from these matrices during pressurization. However, they did not elaborate on how these measurements were made. They further claimed, without providing evidence or further explanation, that the X-rays and light emissions were artifacts of the measurement technique. They reasoned that since the X-rays and light emissions did not correlate with heat production, they were likely of a chemical origin. Yet X-rays cannot be produced by chemical means. However, they can be produced by mechanical means as was demonstrated by Putterman who showed that it was possible to produce X-rays by simply unrolling Scotch tape [25]. Also neutrons and tritium have been measured in experiments done by others that did not correlate with the amount of heat observed [7]. The fact that neutrons, tritium, or X-rays are not commensurate with heat does not mean that they are artifacts. Furthermore, the emission of photons, as well as charged particles and radio frequency signals, have been reported for the D_2 gas loading of polycrystalline Ti [26]. These emissions were attributed to fracto-fusion.

For the Zr–Ni–Pd alloys that were used by NRL, large amounts of heat were generated for both D_2 and H_2 gas loading [24]. While they said the heat was consistent with known chemistry, they did admit that a small amount of heat ($<$ 10% of the total) was unaccounted for and was either due to unidentified chemistry or to measurement error(s). Given the simplicity of their system, it is difficult to ascertain what other chemistries could be occurring. Because they did control experiments that completely balanced out, it is unlikely that the excess heat was due to either measurement errors or instrument malfunctions.

4. NEUTRON DETECTION

The known d + d and d + p nuclear reactions and their energy yields (Q) are d(d,p)t (Q = 4.03 MeV); d(d,n)^{3}He (Q = 3.27 MeV); d(d,γ)^{4}He (Q = 23.85 MeV); d(d,e$^-$)^{4}He (internal conversion, Q = 23.85 MeV); d(p,γ)^{3}He (Q = 5.49 MeV) [27]. Consequently, there were efforts to detect neutrons and tritium. Here we discuss experiments used to detect neutron emissions.

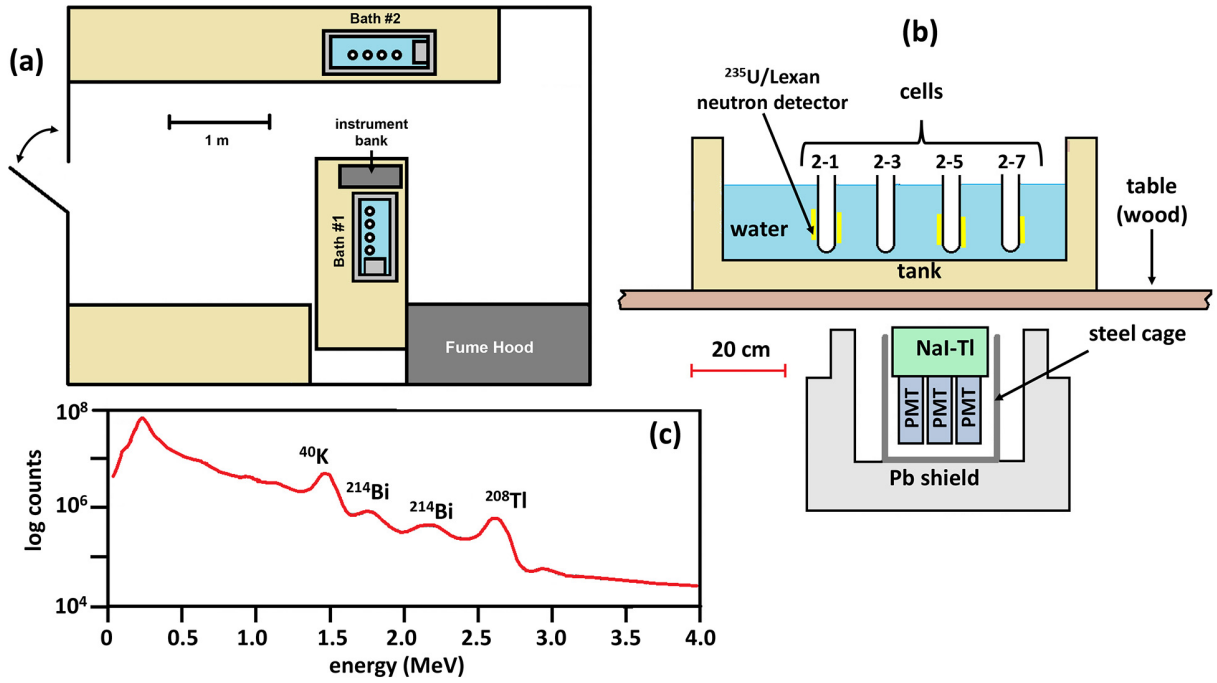

Figure 3. (a) Schematic of the laboratory layout used by Pons and Fleischmann when Salamon *et al*. were conducting their measurements [28]. (b) Side view of the geometry of the electrolytic cells, showing placement of the neutron-detecting sandwiches, and the NaI detector [27]. The electrolytic cells were in bath #1 shown in (a). Cells 2-1, 2-5, and 2-7 have Pd cathodes with diameters/lengths (in cm) of 0.4/1.25, 0.4/10.0, and 0.1/10.0, respectively. Cell 2-3 has a Pt cathode of dimensions 0.1/10.0. (c) Aggregate γ-ray spectrum for 785 h of live collection time obtained using a NaI detector [27]. The dominant background lines are ^{40}K (1.46 MeV), ^{214}Bi (1.76 MeV), ^{208}Tl (2.61 MeV), a backscatter peak ($\sim$0.23 MeV) and a broad peak at $\sim$2.17 MeV due to two lines, ^{214}Bi (2.12 and 2.20 MeV).

4.1. Neutron Detection Using NaI, ^{235}U/Lexan Sandwiches, and HPGe

4.1.1. *Salamon Measurements (University of Utah, U.S.)*

Figure 3a shows a schematic of the Fleischmann–Pons laboratory layout when Salamon e*t al*. conducted their measurements [28]. The schematic shows Dewar-type calorimetric cells with palladium cathodes (one cell contained a platinum cathode) polarized in D_2O solutions. These cells were immersed in thermostat tanks (baths #1 and #2). Several weeks after the press announcement, Pons allowed Salamon's group into the laboratory to make independent measurements of any radiation emanating from the electrolytic cells [27]. A lead-shielded NaI detector (8 in $\times$ 4 in) was placed below the cells, Figure 3b, and collected data nearly continuously for over five weeks in a γ-ray energy range of 0.1–25.5 MeV. In addition, several neutron detectors, comprised of ^{235}U-enriched (80%) foils of unknown thickness sandwiched between nuclear-track-detecting plastic film (Lexan polycarbonate) with and without Cd foil covers, were placed within the water tank adjacent to the cells. The fission capture cross section for ^{235}U is 1.4 barn at 2.5 MeV and 580 barn at thermal energies. Fission fragments will form when ^{235}U nuclei capture 2.45 MeV neutrons formed as a result of the d(d,n)^{3}He reaction. The ^{235}U-neutron interaction to form fission fragments can occur anywhere within the foil. However, only fission fragments formed near the surface of the uranium foil will be able to

leave tracks in the Lexan. Fission fragments formed deeper inside the uranium foil will not be able to exit the uranium and will not be able to create tracks in the Lexan. The absolute neutron detection efficiency of the foil sandwiches was measured using a ^{252}Cf source in a large water tank. The foil sandwiches were placed relative to the source as those used with the electrolysis cells. The measured efficiency was 1.3×10^{-5} fission tracks per emitted neutron and a factor of three lower for those foils with Cd covers. These neutron detectors were used to integrate the neutron flux over a period of approximately three days. Salamon *et al*. said there was no indication of an excess neutron signal from any of the cells, however, according to Pons "no neutron detectors were ever placed in a tank when a cell in that tank was generating excess enthalpy." Today it is known that neutron and tritium production are not commensurate with the excess enthalpy. Furthermore, neutron emission is anti-correlated with excess heat [29].

Salamon *et al*. [27] placed a 8 in $\times$ 4 in NaI detector under the lab bench supporting bath #1, Figure 3b. This detector was used to monitor four open electrolytic cells over a five week period. The γ-ray energy range was 0.1–25.5 MeV. Spectral data were collected nearly continuously during this five week period. While the cells were run in constant-current mode during these five weeks, the current settings were varied. Current densities were not indicated in the Salamon *et al*. paper. However, Pons and Fleischmann [28] later indicated that the cells with Pd cathodes were operating at low current densities but did not indicate what those current densities were. It should be noted that at the time Salamon *et al*. conducted their measurements, the relationship between current density and the observation of either excess heat, tritium production, or neutron emissions was not known. It has since been shown that, in the early Fleischmann–Pons type of experiments, excess heat would be seen for current densities above $\sim$ 100 mA cm^{-2}. Neutron emission and tritium have been seen for current densities near 10 and 70 mA cm^{-2}, respectively [29, 30].

Neutrons resulting from the d(d,n)^{3}He reaction would have an initial kinetic energy of 2.45 MeV and a mean free path in water of 4.9 cm, which decreases to $\sim$0.4 cm as the neutron thermalizes. Because each cell was surrounded by several inches of water, most neutrons emitted would be thermalized and generate a 2.22 MeV γ-ray from the p(n, γ)d reaction. The detection efficiency was measured using an Am-Be neutron source and was found to be 3.0×10^{-3}. Salamon *et al*. [27] obtained individual spectra (an example of which is shown in Figure 3c) by averaging several (10-50) successive spectra to form an aggregate spectrum, which was then subtracted from the original spectrum to form a "residual spectrum." Any transient anomalous signals of duration $<$10–50 h would appear in the residual spectra as positive excesses amidst Poisson fluctuations about zero. Spectra were corrected for temporal variations. The analysis done by Salamon *et al*. on the residual spectra showed no γ-ray signal above background in the 2.2 MeV region.

Given how little was known at the time, the measurements done by Salamon *et al*. were well planned and executed. They had two kinds of detectors to measure neutron emissions. One was a real-time detector that measured the 2.224 MeV γ-ray emitted when a proton captures a neutron. The other was a constantly integrating detector comprised of ^{235}U-enriched foils sandwiched between Lexan. These ^{235}U/Lexan sandwiches were only in contact with the cells for three days. Given the poor sensitivity of these detectors for neutrons, short time of exposure, and the fact that no excess heat was detected during the time the detectors were in contact with the cells, it is not surprising that no fission tracks were observed in the Lexan. Salomon *et al*. did not indicate why they chose to use ^{235}U/Lexan sandwiches for neutron detection. These detectors were developed to monitor reactor neutrons [31]. Another solid state nuclear track detector that could have been used is CR-39 [32]. CR-39 has been widely used for personal neutron dosimetry and is marketed by Landauer as Neutrak®. It covers a broad range of energies: thermal, intermediate, and fast neutrons. CR-39 can come with either a polyethylene radiator or a boron loaded radiator. If a polyethylene radiator is used, tracks are caused by recoil protons produced by the interaction of neutrons with the hydrogen atoms contained in the radiator. The tracks observed in a CR-39 detector with a boron loaded radiator are caused by alpha particles produced from the ^{10}B(n,α)^{7}Li reaction. Another advantage of CR-39 over ^{235}U/Lexan sandwiches is that they can be used to detect 14.1 MeV neutrons resulting from the secondary DT reaction [33,34]. A $\geq$ 9.6 MeV neutron can cause a carbon atom in the detector to shatter into three alpha particles. Triple tracks, in which pits due to three particles are breaking away from a center point, are diagnostic of the t(d, n)α reaction. CR-39 detectors can also be used to estimate the

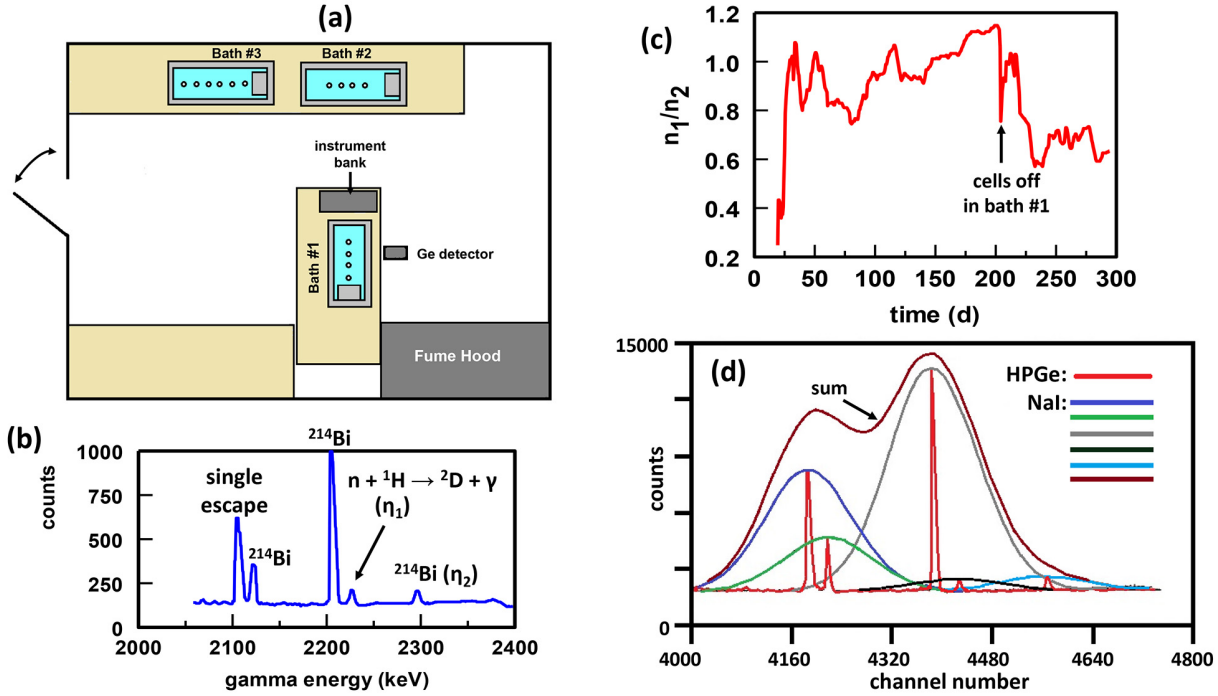

Figure 4. (a) Schematic of the Pons–Fleischmann laboratory layout using an HPGe detector [28]. In bath #1, cells 2-1, 2-5, and 2-7 have Pd cathodes with diameters/lengths (in cm) of 0.8/1.25, 0.4/1.25, and 0.8/1.25, respectively. Cell 2-3 is a Pt blank experiment. (b) A representative γ-ray spectrum obtained 29 days after the cells were turned off [28]. The spectrum was measured using a 33% HPGe detector. Peak assignments are shown. (c) Ratio of the integrated intensities of the 2224 keV (n_1) to the 2293 keV (n_2) bands as a function of time [28]. Current densities of cells in bath #1: 64 mA cm^{-2} days 10 through 155, 256 mA cm^{-2} days 155 through 205, open circuit days 205 through 300. Current densities of cells in bath #3: 64 mA cm^{-2} days 95 through 205, 256 mA cm^{-2} days 205 through 300. (d) Comparison of HPGe and NaI spectra [28]. From left to right, the five most intense peaks are due to a single escape (~2103.5 keV), ^{214}Bi (~2118.6 keV), ^{214}Bi (~2204.1 keV), n + ^{1}H $\rightarrow$ ^{2}D + γ (~2224 keV), and ^{214}Bi (~2293.3 keV). The broad bands are the approximate normalized responses expected for a NaI detector with a resolution of 59 keV. The band labeled 'sum' is the sum of these five normalized contributions, which gives an estimate of the expected response after long-term counting.

energies of neutrons when they actually impact the detector [35], however, these energies will be less than their birth energies.

4.1.2. *Pons and Fleischmann Measurements (University of Utah, U.S.)*

Later Pons and Fleischmann [28] conducted similar measurements as those done by Salamon *et al.* [27]. Rather than using a NaI detector, they monitored their cells using an HPGe detector. Figure 4a shows a schematic of their laboratory setup when they conducted their measurements. While Salamon *et al.* placed their NaI detector under the lab bench, Figure 3b, Pons and Fleischmann oriented the HPGe detector sideways to monitor the thermostat tank as shown in Figure 4a. In their data analysis, Pons and Fleischmann ratioed the integrated intensity of the line due to the n(p, d)γ reaction at 2224 keV (η_1) with that of an adjacent line at 2293.3 keV (η_2) that they attributed to ^{214}Bi. As shown in Figure 4b, these lines have comparable amplitudes. A plot of the η_1/η_2 ratio as a function of time is shown

in Figure 4c. The time dependence of the ratio of the integrated peak intensities from neutron capture in the water bath showed that the excess neutron generation for the polarized Pd cathodes can be detected above the natural cosmic background. A rise in the ratio of the integrated peak intensities was observed when the Pd cathodes in bath #1 were being charged with D^+. On day 205, the polarization of the cells in bath #1 was terminated and a drop in the ratio was observed. The ratio was observed to increase again. Pons and Fleischmann attributed this to neutron generation in the cells in bath #3 since the HPGe detector was not shielded with Pb. Using an Am-Be source, they determined that neutrons were being generated at a level of 5-50 neutrons s^{-1} W^{-1}.

4.1.3. *Comparing Salamon and Pons–Fleischmann Results*

How to explain the discrepancy in the real-time measurements done by both Salamon *et al*. and Pons and Fleischmann? Could it be due to the instrumentation that was used? As was indicated *vide supra*, real time measurements were made by Salamon *et al*. using an NaI detector. While the NaI detectors are very sensitive, they produce low resolution spectra as shown in Figure 3c. In Figure 3c, the spectrum shows three fairly large, broad background peaks between 2.0 and 2.6 MeV which could interfere with the detection of the 2.224 MeV γ-ray. At 2.224 MeV, the resolution of the NaI detector used by Salamon *et al*. was 59 keV. Such a low spectral resolution could make detection of the 2.224 MeV γ-ray difficult. This possibility was addressed by Pons and Fleischmann [28]. Figure 4a shows a schematic of their laboratory setup when they conducted their measurements. Although less sensitive than the NaI detector used by Salamon *et al*., HPGe detectors exhibit higher resolution. Figure 4b shows a γ-ray spectrum obtained by Pons and Fleischmann of operating cells using a HPGe detector (33% efficiency, 1.9 keV resolution) [24]. Compared to the NaI spectrum, Figure 3c, the 2.12 and 2.20 MeV ^{214}Bi lines are completely resolved. Also the ^{214} Bi line at 2.29 MeV is seen in the HPGe spectrum but not the NaI. Figure 4d shows the spectral region of interest for the p(n,γ)d reaction. The HPGe spectrum was measured by Pons and Fleischmann. The five broad bands are the approximate normalized responses expected for an 8in $\times$ 4 in, circular cylinder NaI detector with a resolution of 59 keV. The band labeled "sum" is the sum of the five normalized broad bands and shows the approximate shape of the composite line that would have been measured by the NaI detector. It would be difficult to extract the weak line due to the p(n, γ)d reaction from such a poorly resolved composite band.

4.1.4. *Lead Shielding Interactions*

In their measurements, Salamon *et al*. had surrounded their NaI detector with lead, Figure 3b [27]. They did not indicate how much lead was used to shield the detector. In contrast, the HPGe detector used by Pons and Fleischmann was unshielded [28]. Shielding can affect full energy peak intensities as well as scattering in spectra [36]. When scattering occurs, the continuum is elevated in the spectrum which limits the ability to detect low and mid energy gamma emissions. An experiment done to investigate the feasibility of uranium fissioning using Pd/D co-deposition demonstrated the effects of lead shielding on gamma ray spectra [37]. Figure 5a shows a schematic of the electrochemical cell used in this experiment. The cathode consisted of a 0.25-mm diameter Au wire wrapped around a $\sim$1 cm length of 0.5-mm diameter native uranium wire. This cell was placed inside a lead cave in close proximity to a 10% HPGe detector with a 1.27-mm thick Al window. Figure 5b shows a spectrum obtained for uranium wire using an HPGe detector in a Compton suppressed lead cave. One of the advantages of a Compton suppressed system is a reduction of the background [38-40]. The spectrum for the native uranium wire, Figure 5b, matches that reported for uranium oxide [41]. Peaks due to the ^{235}U and ^{234}Th lines are indicated. The lines between 85 and 116 keV are due to U and Th X-rays. These are stimulated X-rays that are generated by the refilling of the K shell electron orbits ionized by the passage of charged particles or higher energy gamma rays generated by the decay of ^{235}U and ^{238}U [42]. Figure 5c shows spectra of the lead cave and the cell after 19 h of electrolysis at -0.4 mA. The lines seen in both spectra overlap. Although

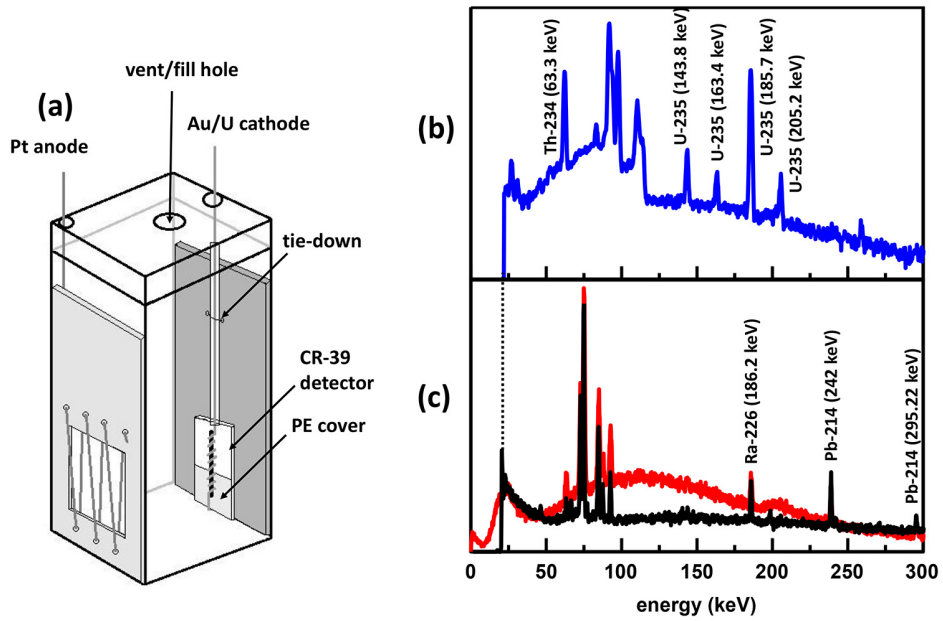

Figure 5. (a) Schematic of the butyrate electrochemical cell used to conduct Pd/D co-deposition on a Au/U composite cathode. (b) Gamma ray spectrum of a native uranium wire obtained using a HPGe detector in a Compton suppressed lead cave [37]. (c) Gamma ray spectra (not time normalized) for the Pb cave (black) and the cell after 19 h of electrolysis at -0.4 mA (red) [37]. The dashed line at ~20 keV indicates the cut off of the Al window of the HPGe detector. Some peak assignments are shown.

a uranium wire is present in the cell and it is radioactive, no peaks due to the stimulated Th/U X-rays are seen nor are the γ-ray lines due to ^{235}U and ^{234}Th. The lines between 59 and 96 keV are due to lead fluorescence of the cave [37]. Broad bands are observed in the spectrum obtained for the electrolytic cell. These broad band are due to neutron scattering within the HPGe detector. The emission of neutrons was verified by triple tracks and fission tracks in the CR-39 detector [37]. The results summarized in Figures 5b and 5c indicate that lead shielding alone could swamp any weak, lower energy emissions. If present, Graded-Z shielding of the lead, comprised of decreasing Z materials, absorbs the lead fluorescence and successively lower Z bremsstrahlung, fluorescence, and Auger electrons.

4.2. D Flux in the Metal Lattice

Initiation of heat production in heavy water electrolysis at palladium cathodes requires simultaneous attainment of four conditions: (i) high loading or chemical potential of D within the Pd lattice; (ii) an initiation time at least ten times longer than the D diffusion time constant (the time constant of diffusion increases with the square of radius); (iii) a minimum or threshold electrochemical surface current or current density that is not correlated to the bulk D loading; and (iv) deuterium flux [43, 44]. The cyclic change in bulk, average loading results from a flux or 'breathing' of deuterons in and out of the metal cathode through its surface. A direct correlation between heat flow and deuterium flux has also been reported between Pd with D_2 reactions in the gas phase [45].

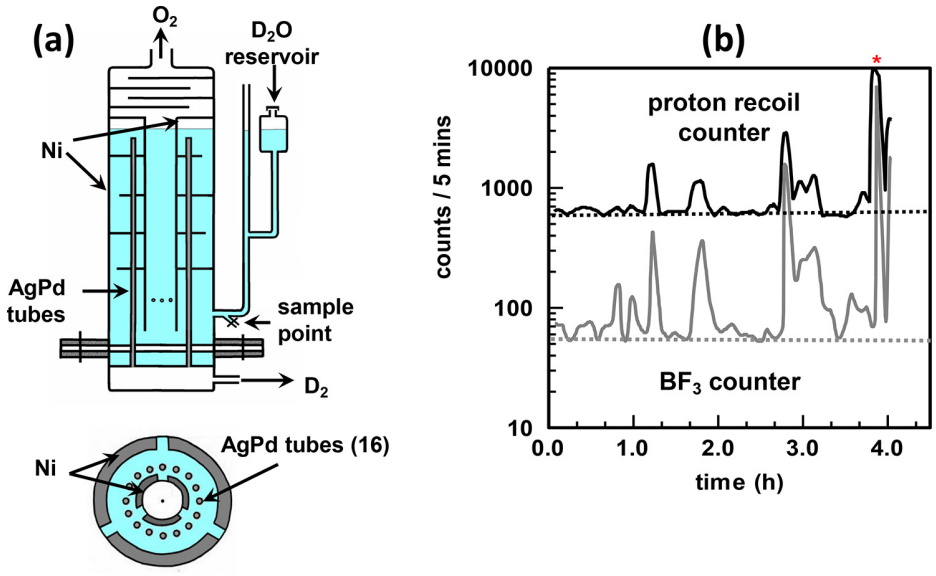

Figure 6. (a) Schematic of a Milton-Roy electrolytic cell used in the BARC experiments [46]. $Ag_{0.25}Pd$ tubes are 200 mm in length and 3 mm in diameter. The electrolyte was 20% NaOD in D_2O. (b) Neutron counts measured as a function of time using a proton recoil counter (top) and a BF_3 counter (bottom) [46]. Dotted lines indicate background count rates for both detectors. The * indicates when the current was set at 100 A.

4.2.1. *BARC (India) Experiments*

Experiments that assured deuterium flux in the metal lattice were done by two different groups. The group in BARC [46] conducted electrolysis experiments using a Milton-Roy electrolytic cell, Figure 6a, which it could operate up to 100 A. The wet surface area of the 16 AgPd alloy tubes was $\sim$ 300 cm^2. During electrolysis, the cell was monitored using two different kinds of neutron detectors. They used BF_3 counters embedded in paraffin blocks for thermal neutron detection and proton recoil plastic scintillator counters for fast neutron detectors. The plastic scintillator counters were also sensitive to high energy gammas. Both the proton recoil and BF_3 detectors were mounted 10 cm from the cell. The background was monitored using a bank of three ^3He counters, embedded in paraffin, which were about 1.5 m from the cell. While monitoring for neutrons, cell current, voltage, and temperature were also recorded and samples were collected for tritium analysis using the liquid scintillation technique. Figure 6b shows the results of the BF_3 and proton recoil neutron detectors during the first run in April of 1989. Clearly the detectors track one another. As the current was slowly increased to 100 A, the cell overheated which caused the trip circuit to turn off cell power. This was followed by a burst of neutrons that was approximately two orders of magnitude larger than background levels over a 2 min interval. Of the 11 cells, six saw a neutron signal within 9 h of operation, one within 24 h, and two showed a neutron signal after 2 weeks. The neutron emissions were observed to stop after continued electrolysis. At the end of this experiment, a sample of the electrolyte was taken and the tritium activity was measured to be 1.5 μCi mL^{-1}. Compared to the initial stock heavy water value of 0.075 nCi mL^{-1}, this high build up by a factor of $\sim$20,000 was far beyond what could be accounted for by electrolytic enrichment alone.

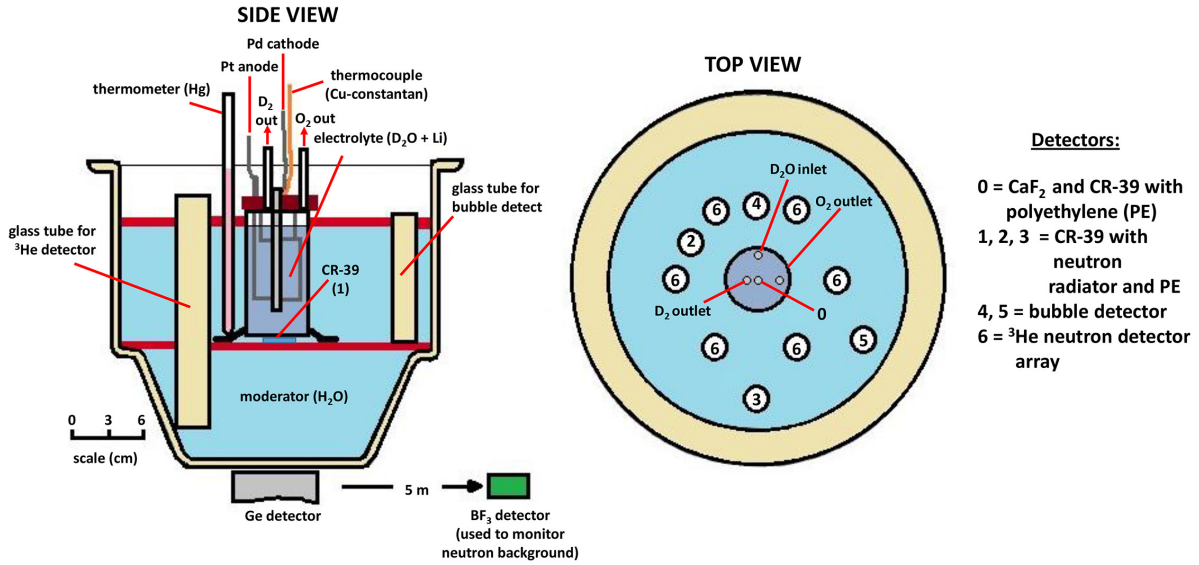

Figure 7. Schematic of the experimental setup used by Ilić *et al*. [47]. The cell with a Pd cathode (tube), a Pt anode (mesh), and 0.1 M LiOD in D_2O electrolyte was placed in a tank with H_2O neutron moderator (side view). Positions of the detectors are indicated.

4.2.2. *J. Stefan Institute, E. Kardelj University (Yugoslavia)*

Ilić *et al*. [47] conducted their own search for neutrons, protons, tritons, ^{3}He ions, and gamma/X-rays during Pd/D electrolysis. Figure 7 shows a schematic of their experimental set up. The Pd cathode was a 10 cm long Pd tube with an outer surface area of 20.4 cm^2. In the cell only 7 cm of the cathode were submerged in the electrolyte. Because the Pd was not fully submerged, the D/Pd loading was considerably less that unity (0.58 for run #1 and 0.48 for run #2). The current density was 25 mA cm^2. The search for neutrons was carried out by an array of six ^{3}He proportional counters, two BD-100 bubble damage polymer detectors, CR-39 track-etch detectors in combination with neutron radiator and polyethylene, and a high purity Ge semiconductor detector. A bare CR-39 track etch detector and CaF_2 thermoluminescent dosimeter were used to detect charged particles. A BF_3 proportional counter placed ~5 m from the cell was used to monitor the neutron background. No statistically significant signal confirming fusion was observed using these nuclear diagnostics. The researchers did not indicate the source of their Pd. Miles had shown that the ratio of success in obtaining excess power varied greatly with the source and batch of Pd used [17]. Also the surface area of the cathode was considerably less than that of the cathodes used in the BARC experiments. This is significant because it is now know that not all sites in the lattice will produce excess heat or emit energetic particles. SEM analysis of Pd cathodes have shown the presence of craters [48]. Many craters show evidence of melting, i.e., smooth surfaces. These craters appear to be due to high power, but very local, energy releases. The presence of new elements, that were not present in the cell components, were associated with these craters and are suggestive of transmutation [49]. These craters show the location of sites that had been active. Likewise autoradiography of several thousand TiD_x chips treated in liquid nitrogen showed that tritium had been produced in only a few chips [50]. But even in those chips tritium production was restricted to a small number of localized "hot spots." Consequently, a larger surface area increases the probability of having LENR-active sites.

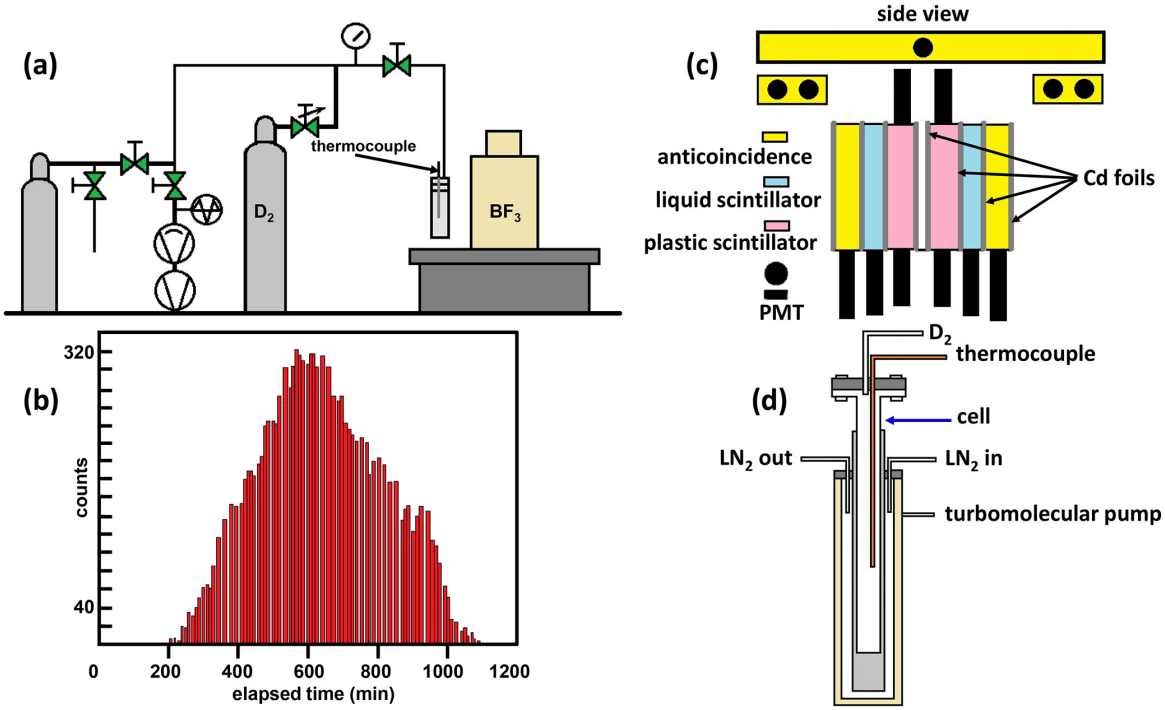

Figure 8. (a) Schematic of the experimental setup used by De Ninno *et al.* in their Ti/D_2 gas loading experiment [51]. (b) Time evolution of neutron emissions during one run [51]. The values indicated are integral counts over periods of 10 min. (c) Detector geometry and composition used by Boragno *et al.* in their Ti/D_2 gas loading experiment [56]. (d) Schematic of the gas loading cell and cryostat used by Boragno *et al.* [56].

4.3. Detection of Neutron Emissions during Ti/D Gas Loading

4.3.1. *ENEA (Italy)*

In 1989, De Ninno *et al.* [51] reported on the emission of neutrons in the Ti/D_2 system. Figure 8a shows a schematic of their experimental setup. About 100 g of Ti shavings were placed in a stainless-steel cell and the cell was connected to a deuterium cylinder through valves and a pressure regulator. A manometer monitored the pressure in the cell and a thermocouple, in contact with the upper part of the Ti shavings, measured the temperature. A Dewar was placed around the cell in order to change the cell temperature between room temperature and liquid-nitrogen temperature. A BF_3 neutron counter with high sensitivity was positioned close to the cell. Figure 8b shows the results of one run. In this run, D_2 had been in contact with the Ti bed, at different temperatures and pressures, for roughly one day. During this time, neutron counts just above the background (2 counts h^{-1}) were detected. The D_2 was evacuated from the system by vacuum pumping and the liquid-nitrogen Dewar was removed allowing the cell and its contents to rise toward room temperature. After three hours into desorption, neutron counts began to increase. The average count in the active period was on the order of 1000 counts h^{-1}. Given the efficiency of the BF_3 detector, the system emitted more than 5000 neutrons s^{-1}.

4.3.2. *Replications*

Attempts [52-56] were made to replicate the results reported by De Ninno *et al*. In these replication attempts, Ti/D_2 samples underwent thermal excursions between 77 K (liquid nitrogen) and room temperature. Different kinds of neutron detectors were used in these experiments. Raj *et al*. [52] used an array of 24 ^{3}He counters (each counter was 50 cm in length, 2.5 cm in diameter, and filled with ^{3}He at 4 atm) arranged in a well like geometry. Counters were housed in paraffin moderators. The Ti metal pieces were cut from a sheet and surface cleaned and subjected to activation treatment before D_2 loading. Most experiments were done in the desorption mode. In some experiments, deuterium pressure was cycled between high and low values by changing the temperature of the cell housing. Bursts of neutrons were observed to occur. After several cycles neutron emissions were observed to cease. Kamm *et al*. [53] used 57 g Ti sponge samples in their experiments. Neutron detection was done using a Reuter-Stokes ^{10}B-lined proportional counter. No neutron emissions were observed. In their experiments, Miljanić *et al*. [54] used a BF_3 detector, a neutron/gamma NE-213 scintillator detector with gamma discrimination, and a track etch proton detector that was taped to the outer surface of the reaction vessel as close as possible to the potential neutron source. Their 40 g of Ti shavings were made from a block of sintered Ti. A 5.45 g Pd tube was also placed in the reaction vessel. Twice in their experiments they saw neutron counts 3–4 times above background that lasted over 1.5 h. The neutron detector developed by Menlove *et al*. [55] consisted of an array of ^{3}He tubes in a CH_2 moderator. The inner ring of the detector array had nine ^{3}He tubes while the outer ring had 42. The sample vessel, containing 300 g of Ti chips (0.5 mm thick and 1.5 mm wide) was placed inside the inner ring. They detected neutron emissions above the background with a significance level of 3 to 9 σ. Figure 8c shows the neutron detection system employed by Boragno *et al*. [56]. Their neutron detector was composed of three cylindrical coaxial scintillator shells. The inner shell was filled with NE-213 liquid scintillator and the outer two were plastic NE-102A. Cd sheets (1 mm thick) were interposed between the scintillators to capture thermalized neutrons. An anticoincidence scintillator was placed on top of the detector to reduce the cosmic ray background. A 30 cm^3 cylindrical sample containing 24 g of Ti, Figure 8d, was inserted in the central hole. They flowed deuterium gas over different samples of Ti shavings and powders. No neutron emissions were detected.

In both De Ninno's original experiment and the subsequent replications, the source of the Ti used was not indicated. It would not be surprising that, like Pd, some sources of Ti would be more LENR active than others. Different morphologies of Ti were used in these experiments. Shavings, chips, powder, and sponge were used. Also the amount of Ti used in the experiments varied from 24 g, used in Borangno *et al*.'s effort [56], to 300 g in Menlove *et al*.'s [55]. It has been shown that the rates of reactions depend on the total area of the lattices in an LENR experiment, the fraction of that area which is active, and the number of reactions per area per second [57]. As was discussed *vide supra*, autoradiography of several thousand TiD_x chips treated in liquid nitrogen showed that tritium had been produced in localized "hot spots" in only a few chips [50]. It stands to reason that the same would have been true for neutron production.

5. CHARGED PARTICLE DETECTION

Efforts were also made by several researchers to detect energetic charged particles using both real-time and integrating detectors. As with the efforts made to detect neutrons, some experiments conducted to detect energetic charged particles were successful while others were not.

5.1. Use of CR-39 to Detect Energetic Charged Particles

CR-39 is a highly cross-linked, thermoset polymer that is inexpensive, chemically resistant, and exhibits both high abrasion and impact resistance. Its most common use is in optics, however, CR-39 is also widely used as a solid-state

nuclear track detector (SSNTD) in the inertial-confinement-fusion (ICF) field to detect the energetic charged particles and neutrons created upon laser compression of the DT fuel capsule [58]. One primary reason for its use is that CR-39 is not affected by the electromagnetic pulse (EMP) that disables electronic detectors in an ICF experiment. Besides cost and ruggedness, other properties that make CR-39 attractive for use in the ICF field are its integrating capability and degree of charge and energy discrimination. It can be used to detect both charged particles and neutrons. Like photographic film and other SSNTD, CR-39 is an example of a constantly integrating detector which means that once an event is detected it will be permanently stamped in the plastic. While it will not be known when the events occurred, the signal will not be averaged away.

5.1.1. *UC Berkeley (U.S.)*

In 1978, the group headed by Buford Price [59] at The University of California in Berkeley was the first to report that CR-39 could be used as an SSNTD. In 1989, they did both D_2 gas loading of Pd and Ti foils as well as electrolytic loading of Pd foils [60]. For the gas loading experiments the 100 μm thick Ti and 233 μm thick Pd foils were cleaned using *aqua regia*. After preloading the foils with deuterium, they were clamped to a CR-39 sheets (contact area 2 cm^2 for each sample) and placed in a stainless-steel pressure cell attached to a source of D_2 gas. After evacuating the cell, it was loaded with D_2 gas to a pressure of 15 bars and underwent thermal excursions between 77 K (liquid nitrogen) and room temperature over a 9 h period. There was no mention of an *aqua regia* treatment of the 25 μm thick Pd foils used in the electrolysis experiments. However, they did indicate that a 100 nm Au diffusion barrier was evaporated on Pd and that this Au barrier side was in contact with the CR-39 detector. Electrolysis was performed at 1.00 mA cm^{-2} for 13 days. For both sets of experiments, there was no significant increase in the number of tracks in the CR-39 detectors. However, linear energy transfer (LET) analysis indicates that 0.82 MeV ^{3}He, 1.01 MeV triton and 3.02 MeV proton would go through 1.156, 4,168, and 31.02 μm of Pd, respectively. Since reactions to create these particles could happen anywhere inside the Pd, only those that occurred near the Pd/CR-39 interface have a greater likelihood of being registered in the CR-39 detector. The sources of the Pd and Ti were not indicated so the foils may not have been LENR active. And it is possible that the treatment with *aqua regia* may have poisoned the surface of the foils. This was address by Li *et al*. [61].

5.1.2. *Tsinghua University (China)*

Li *et al*. [61, 62] did gas loading of Pd foils. After heating Pd foils (0.02 cm $\times$ 0.5 cm $\times$ 2 cm) at 500°C for two hours at 7×10^{-2} Torr, the foils, CR-39 detectors, and CaF_2 thermoluminescent dosimeters (TLDs) were assembled into sandwich like structures. While the CR-39 was selected for charge particle detection, the TLD was chosen to detect electromagnetic radiation. These sandwiches were then placed in a stainless-steel vessel attached to a source of D_2 gas. After evacuating the vessel, it was loaded with D_2 gas to a pressure of 9 atm and immersed in liquid nitrogen for four hours. Then the valve between the vessel and the D_2 gas source was closed and the vessel was allowed to warm to room temperature after the liquid nitrogen vaporized. The cooling/warming cycle was repeated several times over a two day period. Figure 9a shows photomicrographs of CR-39 exposed to D_2 gas, Pd in contact with H_2 gas, and Pd exposed to D_2 gas. As can be seen, tracks were only observed for the Pd/D_2 experiment. While no tracks were observed for the CR-39 detector used in the Pd/H_2 experiment, it exhibited a similar signal of electromagnetic radiation as the Pd/D_2 experiment. The electromagnetic radiation may originate from electrons which are transiting from state to state when palladium foils are filled with hydrogen or deuterium. They then did an experiment where they cleaned the Pd foil with *aqua regia*. [61]. They used this foil in the D_2 gas loading experiment and, like the Berkeley group [60], saw no tracks in the CR-39 detector. Li *et al*. [61] then analyzed the surface of the Pd foil cleaned by *aqua regia* using an auger electron scanning probe and saw a clear peak due to chlorine. Using the argon mill, they found

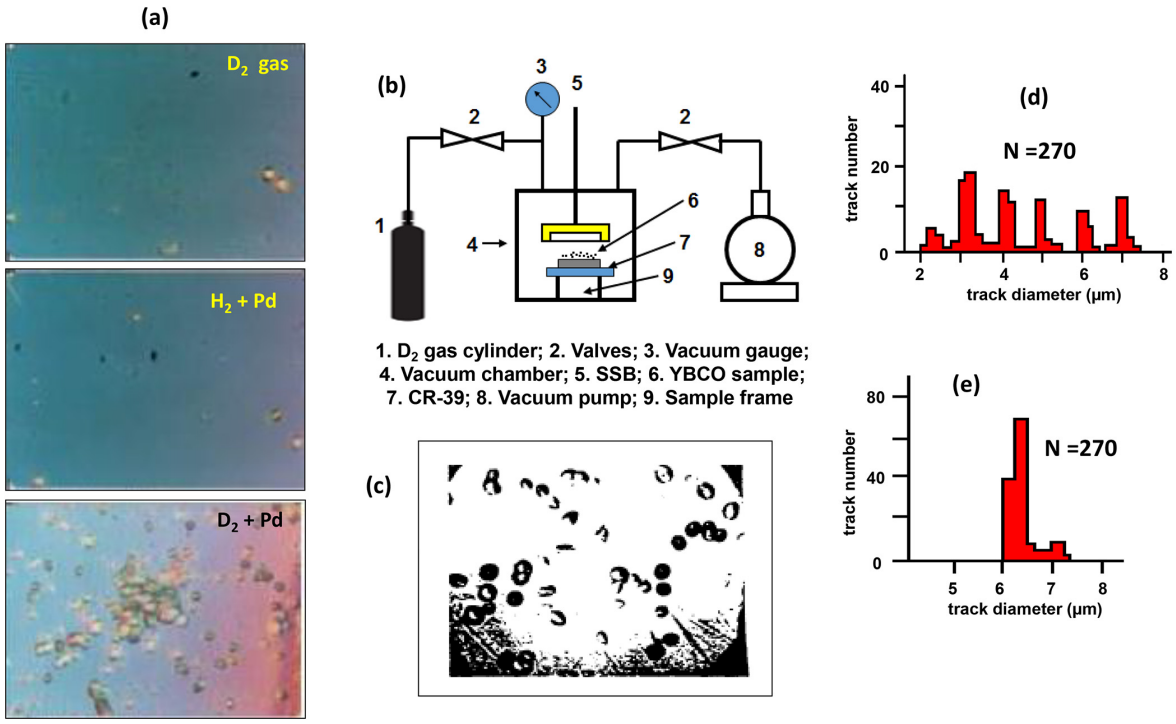

Figure 9. (a) Photomicrographs of tracks in CR-39 exposed to D_2 gas and CR-39 in contact with Pd foil and exposed to either H_2 or D_2 gas [61]. Magnification is 300X. Republished with permission from Xing Zhong Li. (b) Schematic of the experimental setup used by Jin *et al*. [63, 64]. (c) Photomicrograph of tracks on CR-39 produced by $D_xY_1Ba_2O_{7-\delta}$ [58]. (d) and (e) Statistical distribution of circular tracks on CR-39 produced by vertically incident particles for $D_xY_1Ba_2O_{7-\delta}$ and ^{241}Am α-source, respectively [63]. The total number of tracks, N, are indicated.

that the chlorine penetrated into the Pd to a depth of a few hundred angstroms. They then did an experiment where they used chlorine gas to intentionally contaminate the Pd surface. Again they saw no tracks in the CR-39 indicating that surface contamination may suppress the anomalous nuclear effects.

5.1.3. *Graduate School, University of Science and Technology of China*

The high temperature super conductor, $Y_1Ba_2Cu_3O_{7-\delta}$, is able to absorb hydrogen and structural analysis has shown that the absorbed hydrogen is located on the Cu-O plane [63, 64]. In 1993, Jin *et al*. reported on observing an anomalous nuclear effect when $Y_1Ba_2Cu_3O_{7-\delta}$ absorbed deuterium. Figure 9b shows a schematic of the experimental arrangement they used to expose $Y_1Ba_2Cu_3O_{7-\delta}$ pellet or powder to deuterium gas. The $Y_1Ba_2Cu_3O_{7-\delta}$ sample was in direct contact with a CR-39 nuclear track etch detector. An Au-Si surface barrier (SSB) detector was placed above the sample. In their experiment, the chamber was evacuated to about 10^{-1} Pa and then filled with D_2 gas to a pressure of 1 atm. The experiment was terminated after 1 to 2 days of exposure. The CR-39 detector was etched. A photomicrograph of one detector is shown in Figure 9c. After subtracting the background, the track density was 3×10^5 cm^{-2}. Figure 9d shows the size distribution of circular tracks obtained for tracks produced by vertically incident particles in the $D_2/Y_1Ba_2Cu_3O_{7-\delta}$ experiment. For comparison, the size distribution of circular tracks produced by

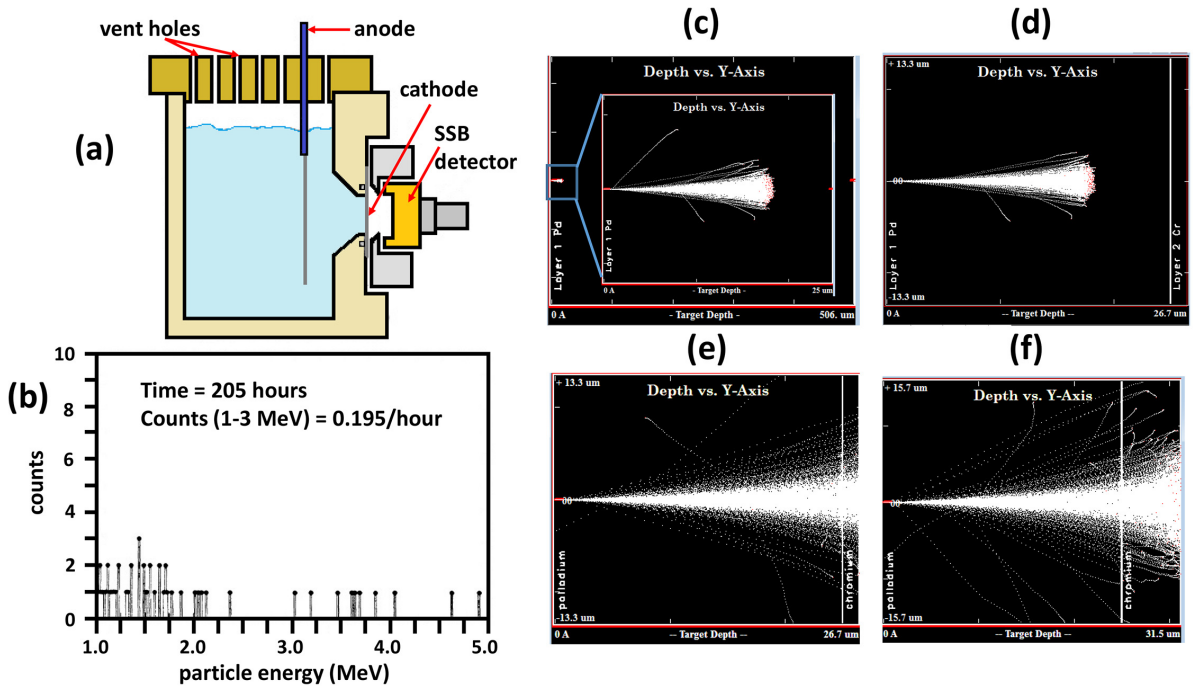

Figure 10. (a) Cross section of the Teflon electrolytic cell used by Ziegler *et al*. [65]. (b) Charged particle spectrum for a thin Pd cathode (25 μm thick, backed with 1.76 μm Au) during 205 h of charging. Results of TRIM calculations for (c) 8 MeV α-particles going through 0. 5 mm thick Pd, 200 Å thick Cr, and 6.5 μm thick Au; (d) 8 MeV α-particles going through 0.025 mm thick Pd, 200 Å thick Cr, and 1.7 μm thick Au; (e) 3.02 MeV protons going through 0.025 mm thick Pd, 200 Å thick Cr, and 1.7 μm thick Au; and (f) 3.02 MeV protons going through 0.025 mm thick Pd, 200 Å thick Cr, and 6.5 μm thick Au.

vertically incident α-particles from an ^{241}Am α-source is shown in Figure 9e. Only one peak, due to the 5.49 MeV α–particle is observed for the CR-39 detector that was exposed to the ^{241}Am source. In contrast, several peaks were observed in the size distribution obtained for the CR-39 detector used in the $D_2/Y_1Ba_2Cu_3O_{7-\delta}$ experiment indicating that several species and/or energies of charged particles were formed. In the absence of D_2 gas, no tracks were observed in the CR-39 detector. Interestingly, Jin *et al*. made no mention of the measurements taken with the SSB. From this we can conclude that either the flux of energetic particles was too low to be detected or the particles formed were neutrons, which would not be detected by an SSB detector.

5.2. Use of SSB to Detect Energetic Charged Particles

5.2.1. *IBM (U.S.)*

In 1989, Ziegler *et al*. [65] constructed electrolytic cells to detect charged particles from d+d fusion reactions using SSB detectors. Figure 10a shows a schematic of the Teflon electrolytic cell. The anode was Pt (2 cm wide and 4 cm long). A thermocouple was attached to the top of the anode. A 7 cm^2 conical hole in the side of the cell led to the 2 cm^2 Pd cathode of various thicknesses (0.025 to 0.5 mm). A dense 1.7-6.5 μm Au film was sputtered on the backside of the Pd. A 200 Å layer of Cr was used to adhere the Au to the Pd. While the anode–cathode spacing was adjustable,

a spacing of 2 cm was used in these experiments. To measure charged particles an SSB was placed $\sim$ 2 mm away from the cathode. The SSB was optimized to detect charged particles up to about 8 MeV. Particles with energies above this would still be detected but some energy information would be lost. The Teflon cell held $\sim$150 cm^3 of electrolyte. The electrolyte consisted of 0.1 M LiOD in various mixtures of H_2O and D_2O. The anode/cathode current density was held at 150 mA cm^{-1} for all studies. No excess heat or nuclear fusion products were detected for any of the samples tested. Figure 10b shows a charged particle spectrum obtained for a thin Pd cathode. A background spectrum was obtained by turning off the cell current. The resultant spectrum was virtually identical to that obtained while the cell was operating.

There are several possible reasons why no charged particles were detected by the SSB in the Ziegler *et al*. experiments. In their publication they indicate that the Pd that was used was 99.9% pure [65]. However, the source of the Pd was not indicated and, has been discussed *vide supra*, not all Pd is LENR active. The fact that no heat was detected using the thermocouple attached on the top of the Pt anode indicates that the Pd was not LENR active. TRIM (TRansport of Ions in Matter) [66] calculations of 8 MeV protons, 8 MeV alphas, and 3.02 MeV protons through the cathodes used by Ziegler *et al*. were done. The cathodes used by Ziegler *et al*. had three layers—Pd (0.025-0.5 mm thick), Cr (200 Å thick) and Au (1.7-6.5 μm thick). Plots of some of these calculations are shown in Figures 10c–f. Charged particle formation can occur anywhere inside the lattice but in these calculations the charged particle is formed at the surface of the Pd in contact with the electrolyte. These charged particles can also travel through the lattice in any direction—forward, backwards, and sideways. Particles traveling sideways or backwards away from the SSB will not be detected. In these calculations we only looked at particles that were traveling in the forward direction towards the SSB. For 0.5 mm thick Pd, calculations show that the 8 MeV protons and alphas cannot exit the cathode unless they were formed very close to the Pd/Cr interface, Figure 10c. The same would be true of 3.02 MeV protons. For 25 μm thick Pd, 8 MeV protons will go through but an 8 MeV α formed at the cathode/electrolyte interface will not, Figure 10d. However, this calculations shows that if the 8 MeV alpha formed deeper inside the cathode near the Cr/Au layers ($\geq$ 8.4 μm from the cathode/electrolyte/interface), it could go through and impact the SSB. Calculations done for 3.02 MeV protons indicate that these protons can go through a 25-μm thick Pd foil, 200 Å Cr film, and 1.7–6.5 μm Au film. If the Pd foil had been LENR active, the d(d,p)t reaction does not correlate with the heat and is a minor secondary reaction.

Another consideration is D flux and cathode reaction surface area both discussed *vide supra*. The cathodes prepared by Zeigler *et al*. had an Au film sputtered on the side that faced the SSB. This Au film will impact D flux through the lattice. The surface area of the Ziegler *et al*. cathodes was 2 cm^2 and they detected no energetic charged particles. In the neutron detection experiments done at BARC [46] and by Ilić *et al*. [47], the surface areas of the cathodes were 300 and 20.4 cm^2, respectively. While neutrons were detected in the BARC experiments none were detected in the Ilić *et al*. experiments. Furthermore the autoradiography of TiD_x chips discussed *vide supra* showed small numbers of localized "hot spots" where tritium production had occurred [50]. This is likely true for Pd as well as evidenced by crater formation in cathodes that produced heat [48]. If so, the rate of proton production may be too low to detect by an SSB in real time.

5.3. X-ray/γ-ray Detection of Energetic Particles

Attempts have been made to detect charged particles using X-ray and γ-ray detectors. One such effort was made by Salamon *et al*. [27]. There had been reports of excess tritium production [46, 50, 67]. The most likely source of tritium in the fusion channel d(d,p)t which would occur inside the Pd lattice. Salamon *et al*. [27] explored Coulomb excitation [68] to detect these protons. Given the configuration of the experiment, shown in Figure 3a and b, this was probably the only way feasible to measure these protons. Coulomb excitation is a process of inelastic scattering in which a charged particle transmits energy to the nucleus through the electromagnetic field [69]. This process can happen at a much lower energy than that necessary for the particle to overcome the Coulomb barrier and is shown schematically in

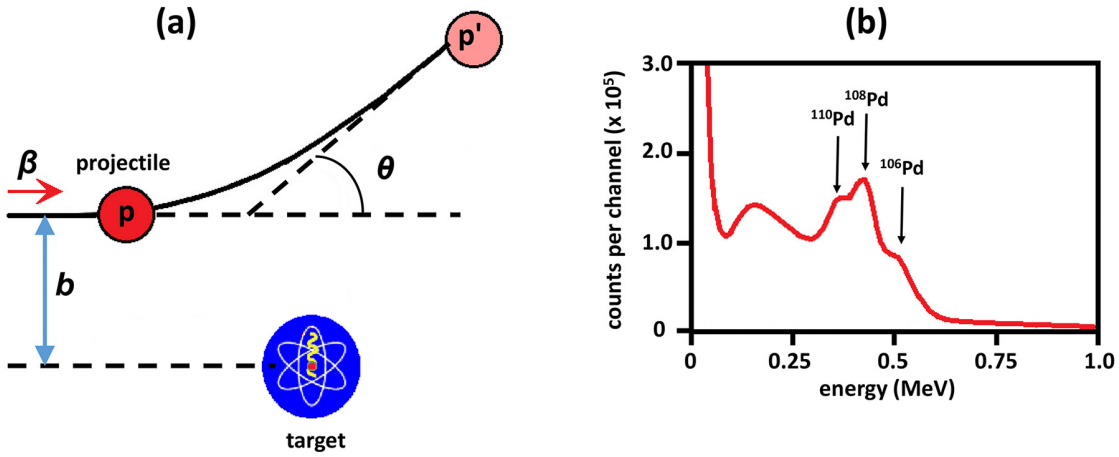

Figure 11. (a) Schematic illustration of a projectile, p, being scattered in the Coulomb field of an infinitely heavy target nucleus [69]. For a given beam velocity β, the impact parameter b depends on the scattering angle θ. (b) Electric-quadrupole (E2) γ-ray lines from the isotopes of Pd, excited by 3.02 MeV protons, as measured by a 3 x 3 in NaI detector [27]. The three lines at 0.37, 0.43, and 0.51 MeV are assigned to ^{110}Pd, ^{108}Pd, and ^{106}Pd, respectively.

Figure 11a [69]. The range of a 3.02 MeV proton is $\sim$ 31 μm. As they traverse through the Pd, the 3.02 MeV protons will cause Coulomb excitation of the even-numbered isotopes of Pd resulting in the spectrum shown in Figure 11b [27]. No signal was observed as Salamon *et al.* [27] monitored the cells during electrolysis in the Pons–Fleischmann laboratory.

To obtain the spectrum shown in Figure 11b, a 3-mm target of natural Pd was exposed to a beam of 3.02 MeV protons generated by a Van de Graaff accelerator. The flux of protons to generate this spectrum was not indicated. To generate $\geq$ 3 MeV protons, Van de Graaff accelerators operate anywhere from 0.2 μA to 3 mA [70]. This current is proportional to the rate at which the protons are generated. Using the lower value of 0.2 μA, the generation rate of protons would be 1.25×10^9 particles s^{-1} (pps). Such generation rates have not been observed in the Pd/D system. As was discussed *vide supra*, BARC [46] measured a $\sim$20,000 increase in their tritium activity (initial and final tritium activities were 0.075 nCi mL^{-1} and 1.5 μCi mL^{-1}, respectively). Tritium, from the d(d,p)t channel, showed an activity of 1.5 μCi that is equivalent to 5.55×10^4 decays s^{-1}—more than four orders of magnitude lower than the protons generated at the lowest setting of a Van de Graaff accelerator (0.2 μA). Other measurements of tritium activity for Pd/D electrolytic cells were significantly lower than what was reported by BARC. Consequently, it is highly unlikely that it would have been possible for Salamon *et al.* to measure 3.02 MeV protons in real time using this method of Coulomb excitation.

Attempts were made to detect Pd X-rays resulting from the refilling of the K shell electron orbits ionized by the passage of charged particles through the Pd lattice. Both Bennington *et al.* [71] and Deakin *et al.* [72] used lithium drifted silicon, Si(Li), detectors to detect these X-ray emissions in real time. A schematic of the electrolytic cell used by Bennington *et al.* [71] is shown in Figure 12a. The cell had a thin Mylar window. The Pd disc cathode was 1.5 mm thick and 20 mm in diameter. A gap between the Pd cathode and Mylar window was less than 1 mm. A peristaltic pump was used to circulate the electrolyte to prevent the trapping of gas bubbles between the cathode and the Mylar window. As shown in Figure 12a, the Si(Li) detector was placed on the other side of the window so that only a small amount of electrolyte and Mylar separated it from the possible source. They estimated that the absorption of the Pd K shell X-rays by water, Mylar, and air would be 6%. A calibration run was performed by placing a 150 nCi ^{241}Am

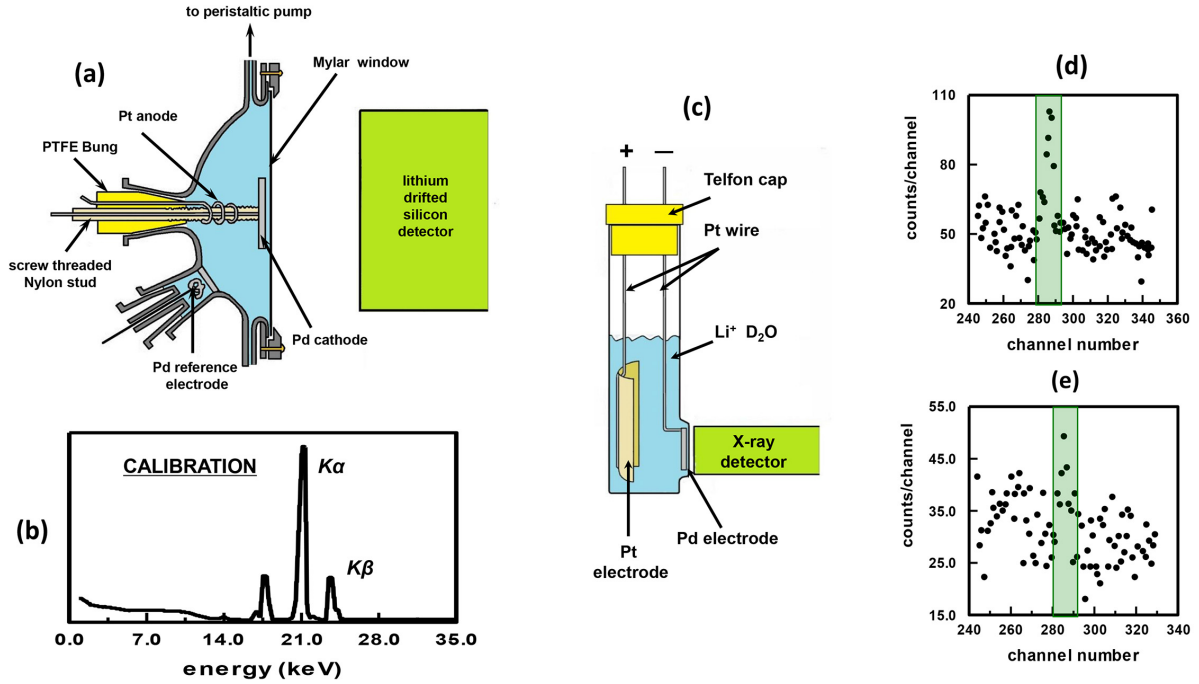

Figure 12. (a) Schematic of the thin walled electrolytic cell used by Bennington *et al*. [71] to look for X-rays in palladium when electrolytically charged with deuterium. (b) A calibration run using a 150 nCi α source in contact with the back of a 0.1 mm Pd foil [71]. The Pd Kα and Kβ lines of Pd are indicated. (c) Schematic of the electrolytic cell used by Deakin *et al*. [72]. X-ray spectra measured when the Pd foil was irradiated with a Ba X-ray source (d) and after 333 h of electrolysis (e). The Pd X-ray line was in the background.

α source against a 100μm thick Pd foil that was in contact with the Si(Li) detector. The resultant spectrum is shown in Figure 12b. A schematic of the cell used by Deakin *et al*. [72] is shown in Figure 12c. This cell was constructed of Pyrex glass with a thin blown Pyrex window. The Pd foil cathode was 50 μm thick and had an area of 1 cm^2 and was pressed against the thin Pyrex window. As shown in Figure 12c, the Si(Li) X-ray detector was placed on the other side of the thin Pyrex window. To demonstrate that Pd K shell X-rays could be detected, a Ba X-ray source was used to stimulate the emission of these Pd K shell X-rays, Figure 12d. It was also shown that the room background radiation caused the Pd cathode to fluoresce and a weak line due to Pd K shell X-rays was present as an artifact in the background, Figure 12e. It should be noted that in both sets of experiments no X-rays above background were detected.

As was discussed *vide supra*, Li *et al*. [61] had demonstrated that Pd/D_2 produced energetic particles using CR-39 detectors. Likewise Mosier-Boss *et al*. [73] also used CR-39 detectors to register energetic particles in Pd/D co-deposition experiments. The main difference between CR-39 detectors and Si(Li) detectors is that the former is a constantly integrating detector and the latter operates in real-time. Forsley *et al*. [74] conducted experiments to investigate this apparent discrepancy between the two kinds of detectors in measuring energetic particles in LENR experiments. In one set of experiments, they placed a 1 μCi ^{241}Am source in contact with a 25-μm thick Pd foil. Using an HPGe detector with a Be window, they obtained a spectrum of the Pd Kα and Kβ X-ray lines. They then placed a 560-μm thick Cu sheet between the Pd foil and the ^{241}Am source. A Cu sheet of this thickness will prevent

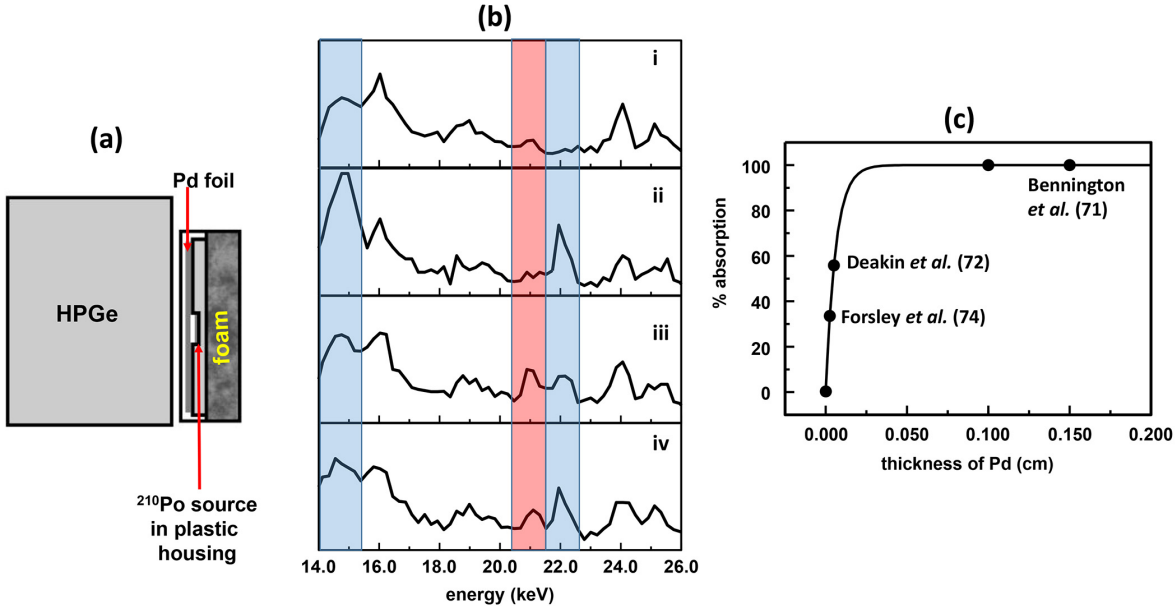

Figure 13. (a) Schematic showing the orientation of the Pd foil, ^{210}Po source, and HPGe used to obtain the spectra shown in (b) [74]. (b) ^{210}Po-Pd experiments conducted by placing the samples in a Pb cave and in direct contact with the HPGe detector where: i = Pd foil, ii = ^{210}Po source, iii = Pd foil in contact with ^{210}Po source, iv = a 100 μm thick acrylic film is between the Pd foil and the ^{210}Po source. Spectra are time-normalized [74]. The blue bars indicate the gamma lines of the unknown contaminant(s) and the red bar indicates the Pd Kα shell X-ray. (c) Plot of the % absorption of Pd X-rays as a function of Pd thickness. The thicknesses of the Pd foils used by Bennington *et al*. [71], Deakin *et al*. [72], and Forsley *et al*. [74] are indicated.

the ^{241}Am α particles from reaching the Pd foil. However, they still observed the Pd Kα and Kβ X-ray lines in the spectrum indicating that something else, that was much more penetrating than the ^{241}Am α particles, was stimulating the emission of the Pd X-ray lines. Besides emitting α particles, ^{241}Am emits a γ-ray at 59.54 keV [75]. It was observed that when the ^{241}Am source was in contact with the Pd foil, the intensity of this γ-ray decreased indicating that it was being absorbed by the Pd foil. This, and the fact that γ-rays are more penetrating than α-particles, indicates that the stimulation of the Pd X-ray lines is primarily due to the 59.54 keV γ-ray.

Forsley *et al*. [74] repeated the experiments using a 0.1 μCi ^{210}Po source in place of the ^{241}Am source. Figure 13a is a schematic of the experimental arrangement used to obtain the spectra in Figure 13b. Figure 13b(i) shows the spectrum of the 25-μm thick Pd foil. A small peak due to the Pd Kα is observed. This peak is due to background radiation stimulating the emission of the Pd Kα X-ray line. The spectrum of the ^{210}Po source is shown in Figure 13b(ii). ^{210}Po is supposed to be a pure α source [75]. However, as can be seen there are two lines at 14.8 and 21.9 keV due to an unidentified contaminant(s) in the source. Another line due to a contaminant(s) was also seen at 122 keV (not shown) [74]. Figure 13b(iii) is the spectrum obtained when the ^{210}Po source was in contact with the Pd foil. Emission of the Pd Kα line is stimulated by the background, the ^{210}Po α particles, and the γ-rays (primarily the 122 keV line) from the unknown contaminant(s). To eliminate the contribution of the ^{210}Po α particles, a 100 μm thick acrylic film was placed between the Pd foil and the ^{210}Po source. The resultant spectrum is shown in Figure 13b(iv). Assuming that the background, ^{210}Po α particles, and unknown γ-rays contribute additively to the Pd Kα X-ray emissions of the Pd - ^{210}Po sample, the peak area due to the ^{210}Po α particles is 1.163×10^{-4} and, for a 0.1 μCi source, this is

proportional to 3700 decays s^{-1}. This rate of particle production is more than two orders of magnitude greater than has been observed from the CR-39 experiments [61, 73]. Consequently, the increase in peak area due to such a low rate of particle production would be too low to see in the measured spectrum.

Self-absorption may be another reason why no emissions above background were observed in the electrolysis experiments. In the experiments done by Deakin *et al*. [72] and Forsley *et al*. [74], the background radiation stimulated the emission of Pd Kα X-rays. In contrast the background radiation did not stimulate the emission of Pd Kα X-rays in the Bennington *et al*. [71] experiment. The cathode used by Bennington *et al*. was 1.5-mm thick while those used by Deakin *et al*. and Forsley *et al*. were 50 and 25 μm thick, respectively. The % X-rays absorbed as a function of Pd thickness was calculated and plotted in Figure 13c [74]. From this it can be seen that the 50 μm thick foil used by Deakin *et al*. would absorb 55.8% of the X-rays while that used by Bennington *et al*. will absorb 100%. It is interesting to note that to obtain the spectrum shown in Figure 12b Bennington *et al*. [71] irradiated a 0.1 mm thick Pd foil with an ^{241}Am α source and not the 1.5 mm thick Pd cathode used in the electrolysis experiment. A 0.1-mm thick Pd foil would have absorbed 80% of the Pd X-rays.

6. CONCLUSIONS

On November 8, 1989, John Huizenga submitted the Final Report of the Cold Fusion Panel [76] to the Energy Research Advisory Board (ERAB) of the DoE. This report was a culmination of members of the Panel participating in the Workshop on Cold Fusion in Santa Fe, NM; visiting several laboratories; examining many published articles and preprints; and participating in many discussions over a six month period. The report indicates that they visited the Pons–Fleischmann and Wadsworth laboratories at the University of Utah; the Jones laboratory at Brigham Young University; the Appleby, Martin, and Bockris laboratories at Texas A&M University; the Lewis laboratory at Caltech; the Huggins laboratory at Stanford University; and McKubre of SRI International (at EPRI). The report also indicated that detailed queries were made of other investigators by telephone. However, the ERAB committee failed to visit Martin Fleischmann, the main scientist behind the Cold Fusion discovery. Some of the negative and positive results discussed in this communication were referenced in this final report. The members of the Panel seem to have taken the experimental results at face value and did not question how the experiments were carried out, the instrumentation used, or the data analysis. As has been discussed in this communication some of the early experiments that gave negative results were seriously flawed. Based on the examination of published reports and several site visits, the Panel concluded that there was no convincing evidence that the excess heat produced in calorimetric cells would be useful sources of energy nor was there convincing evidence to associate the reported heat with a nuclear process. These conclusions were based on the discrepancy between the claims of heat production and the failure to observe commensurate levels of fusion products, which should be by far the most sensitive signatures of fusion. *The Panel further said that cold fusion should not be possible based on established theory*. This goes against Kolthoff's adoption of his advisor, Schoorl's, adage towards research [77], "Theory guides, experiment decides." There is supposed to be a synergistic relationship between theory and experiment. A theory is usually expected to explain existing experimental results and to predict new results, while an experiment is usually expected to check the validity of existing theories and to gather data for modifying them [78].

In the preamble of their 1989 final report [76], the Panel said, "Ordinarily, new scientific discoveries are claimed to be consistent and reproducible; as a result, if the experiments are not complicated, the discovery can usually be confirmed or disproved in a few months. The claims of cold fusion, however, are unusual in that even the strongest proponents of cold fusion assert that the experiments, for unknown reasons, are not consistent and reproducible at the present time." The lack of reproducibility is not unusual in a newly emergent field. This was particularly true of the semiconductor industry. The parallels between irreproducibility in cold fusion and transistors/integrated circuits has been well documented by Rothwell [79, 80]. Today there is great concern over reproducibility in biomedical research

[81-83]. For better or for worse, experimental reproducibility is the coin of the scientific realm. Loscalzo [83] summed up the situation with the following:

From a more practical perspective, reproducibility is a means by which to reduce the tentative nature of an initial scientific observation. The implicit assumptions of tests of reproducibility are that if an initial observation is found to be reproducible, then it must be true; and if an initial observation is found not to be reproducible, then it must be false. While the logic of these concepts is unimpeachable, *we should not conflate scientific truth and reproducibility*. As Jonah Lehrer pointed out recently, "Just because an idea is true doesn't mean it can be proved. And just because an idea can be proved doesn't mean it's true. When the experiments are done, we still have to choose what to believe [84]."

Interestingly, the Panel in 1989 [76] acknowledged that neutrons near background levels had been reported in some D_2O electrolysis and pressurized D_2 gas experiments, but at levels 10^{12} below the amounts required to explain the experiments claiming excess heat if one assumes conventional high temperature deuterium plasma fusion. Significant contemporaneous and subsequent research suggests other factors come into play [85]. This communication has discussed some of those experimental results. However, the Panel [76] concluded that "Although these experiments have no apparent application to the production of useful energy, they would be of scientific interest, if confirmed." One does not expect electrolysis or gas pressurization experiments to produce neutrons. Where was the scientific curiosity to elucidate why or how these neutrons were produced?

As was discussed in this communication, we have a better understanding as to why LENR/cold fusion results have been hard to replicate and we can explain why so many scientists failed in their attempts. Not all samples of Pd or Ti are equal. Even if a given sample of Pd or Ti has the potential of being LENR active, certain conditions, *i.e.* high D-loading and high D flux within the lattice, must be met in order to induce the effect. Furthermore, not all sites within the metal are going to be active. Yet, not knowing any of this and after only six months of investigation, the Panel in 1989 declared that the phenomenon would not be a useful energy source. In 1989, experiments were being conducted using relatively small samples. The technology was nascent and more research was needed to understand the phenomenon before it could be turned over to the engineers for scale up to make a practical energy source. Without this research, it is not possible to gauge how much power LENR could potentially generate once the conditions to initiate the effect have been optimized. In the time since the 1989 DoE report, we have learned more about the metallurgy of Pd and have developed metallurgical treatments that facilitate absorption and hydrogen mass transfer into the Pd lattice [86-88]. It is expected that, given time and resources, we would have learned how to process the metal to make more sites that are LENR-active and to increase the reproducibility. Additional work would have been done to optimize triggering methods. As it is we have learned that magnetic fields [89-91], additives [90] and laser-excitation [90, 92-94] can stimulate the effect. That we have come this far without the necessary funding and resources is a testament to the fortitude and dedication of scientists worldwide who have conducted LENR research.

References

[1] 1989-March 23-Cold Fusion Press Conference at University of Utah; https://www.youtube.com/watch?v=6CfHaeQo6oU

[2] Beaudette, C. G. (2002), Excess Heat & Why Cold Fusion Research Prevailed, South Bristol, Maine: *Oak Grove Press*. https://www.lenr-canr.org/acrobat/BeaudetteCexcessheat.pdf

[3] Mallove, E. (1991), Fire from Ice: Searching for the Truth Behind the Cold Fusion Furor, London: *Wiley*. https://www.lenr-canr.org/acrobat/MalloveEfirefromic.pdf

[4] Krivit, S. B. (2016), Fusion Fiasco (Exploration in Nuclear Research Book 2), San Rafael, California: *Pacific Oaks Press*.

[5] Fleischmann, M.; Miles M. (2018) Letters from Martin Fleischmann to Mel Miles, *LENR-CANR.org*. https://www.lenr-canr.org/acrobat/Fleischmanlettersfroa.pdf

[6] Fleischmann, M.; Pons, S. (1989), "Electrochemically Induced Nuclear Fusion of Deuterium", *Journal of Electroanalytical Chemistry,* **261** (2A): 301–308. https://www.lenr-canr.org/acrobat/Fleischmanelectroche.pdf

[7] Krivit, S.B.; Marwan, J. (2009) "A New Look at Low-Energy Nuclear Reaction Research," *J. Environ. Monit.* **11**: 1731-1746. https://www.lenr-canr.org/acrobat/KrivitSanewlookat.pdf
[8] Miles, M.; Fleischmann, M. (2008) "Isoperibolic Calorimetric Measurements of the Pons-Fleischmann Effect," *Proceedings of ICCF-14*, Washington DC. https://www.lenr-canr.org/acrobat/MilesMisoperibol.pdf
[9] Miles, M.H. (2014) "Examples of Isoperibolic Calorimetry in the Cold Fusion Controversy," *Journal of Condensed Matter Nuclear Science* **13**: 392-400. https://www.lenr-canr.org/acrobat/BiberianJPjcondensedl.pdf#page=402
[10] Rothwell, J. (2020) "Review of the Calorimetry of Fleishmann and Pons," *LENR-CANR.org*. https://www.lenr-canr.org/acrobat/RothwellJreviewofth.pdf
[11] Melvin Miles, personal communication.
[12] Miles, M.H. (2017) "The Fleischmann-Pons Calorimetric Methods, Equations and New Applications," *J. Condensed Matter Nucl. Sci.* **24**: 1-14. https://www.lenr-canr.org/acrobat/BiberianJPjcondensedw.pdf#page=13
[13] Rothwell, J. (2012) "How Nature Refused to Re-examine the 1989 CalTech Experiment," *LENR-CANR.org*. https://www.lenr-canr.org/acrobat/RothwellJhownaturer.pdf
[14] Mallove, E. (1999) "MIT and Cold Fusion: A Special Report," *Infinite Energy* **4** (24): 64-80. https://www.lenr-canr.org/acrobat/MalloveEmitspecial.pdf
[15] Miles, M.H. (2000) "Calorimetric Studies of Palladium Alloy Cathodes Using Fleischmann-Pons Dewar Type Cells." *Proceedings of ICCF8*, Lerici (La Spezia), Italy. https://www.lenr-canr.org/acrobat/MilesMcalorimetrb.pdf
[16] Miles, M.H. (2000) "Report on Calorimetric Studies at the NHE Laboratory in Sapporo, Japan," *Infinite Energy* **5** (30): 22-25. https://www.lenr-canr.org/acrobat/MilesMreportonca.pdf
[17] Miles, M.; Bush, B.F.; Johnson, K.B. (1996) "Anomalous Effects in Deuterated Systems, Final Report," *NAWCWPNS TP 8302*, Naval Air Warfare Center Weapons Division. https://www.lenr-canr.org/acrobat/MilesManomalousea.pdf
[18] Little, S.R.; Luce, G.A.; Little, M.E. (2008) "MOAC – A High Accuracy Calorimeter for Cold Fusion Studies," *Proceedings of ICCF14*, Washington D.C., USA.
[19] Bush, B.F.; Lagowski, J.J.; Miles, M.H.; Ostom, G.S. (1991) "Helium Production During the Electrolysis of D_2O in Cold Fusion Experiments," *J. Electroanal. Chem.* **304**: 271-278. https://www.lenr-canr.org/acrobat/BushBFheliumprod.pdf
[20] Miles, M.H.; Hollins, R.A.; Bush, B.F.; Lagowski, J.J.; Miles, R.E. (1993) "Correlation of Excess Power and Helium Production during D_2O and H_2O Electrolysis using Palladium Cathodes," *J. Electroanal. Chem.* **346**: 99-117. https://www.lenr-canr.org/acrobat/MilesMcorrelatio.pdf
[21] Case, L.C. (1998), "Catalytic Fusion of Deuterium into Helium-4," *in Proceedings of ICCF-7 International Conference on Condensed Matter Nuclear Science*. Vancouver, Canada. https://www.lenr-canr.org/acrobat/CaseLCcatalyticf.pdf
[22] McKubre, M.; Tanzella, F.; Tripodi, P.; Hagelstein, P. (2000), "The Emergence of a Coherent Explanation for Anomalies Observed in D/Pd and H/Pd Systems: Evidence for ^4He and ^3He Production," *in Proceedings of ICCF-8 International Conference on Condensed Matter Nuclear Science*. Bologna, Italy. https://www.lenr-canr.org/acrobat/McKubreMCHtheemergen.pdf
[23] Kidwell, D.A.; Knies, D.L.; Grabowski, K.S.; Dominguez, D.D. (2009), "Yes, Virginia there is Heat, but It is Likely of Chemical Origin," *in Proceedings of ICCF-15 International Conference on Condensed Matter Nuclear Science*. Rome, Italy. https://www.lenr-canr.org/acrobat/ViolanteVproceeding.pdf#page=144
[24] Kidwell, D.A.; Imam, M.A.; Dominguez, D.D. (2012) "Fabrication, Characterization, and Evaluation of Excess Heat in Zirconium-Nickel-Palladium Alloys," *J. Condensed Matter Nucl. Sci.* **8**: 208-218. https://www.lenr-canr.org/acrobat/BiberianJPjcondensedg.pdf#page=214
[25] Chang, K. (2008) "Scotch Tape Unleashes X-Ray Power,: *New York Times*. https://www.nytimes.com/2008/10/28/science/28xray.html
[26] Dickinson, J.T.; Jensen, L.C.; Langford, S.C.; Ryan, R.R.; Garcia, E. (1990) "Fracto-Emission from Deuterated Titanium: Supporting Evidence for a Fracto-Fusion Mechanism," *J. Mater. Res.* **5**: 109-122.
[27] Salamon, M.H.; Wrenn, M.E.; Bergeson, H.E.; Crawford, K.C.; Delaney, W.H.; Henderson, C.L.; Li, Y.Q.; Rusho, J.A.; Sandquist, G.M.; Seltzer, S.M. (1990) "Limits on the Emission of neutrons, γ-Rays, Electrons and Protons from Pons/Fleischmann Electrolytic Cells," *Nature* **344**: 401-405.
[28] Pons, S.; Fleischmann, M. (1992) "Concerning the Detection of Neutrons and γ-Rays from Cells Containing Palladium Cathodes Polarized in Heavy Water," *Il Nuovo Cimento* **105A**: 763- 771.
[29] Hagelstein, P.L.; Melich, M.E.; Johnson, R. (2008) "Input to Theory from Experiment in the Fleischmann-Pons Effect," *in Proceedings of ICCF-14 International Conference on Condensed Matter Nuclear Science*. Washington, DC. https://www.lenr-canr.org/acrobat/Hagelsteininputtothe.pdf

[30] Dr. Peter Hagelstein, MIT, personal communication.
[31] Rago, P.F.; Goldstein, N.; Tochilin, E. (1970) "Reactor Neutron Measurements with Fission Foil-Lexan Detectors," *Nucl. Appl. Technol* **8**: 302-309.
[32] https://www.landauer-fr.com/en/knowledge/go-further/cr-39-technology/
[33] Mosier-Boss, P.A.; Szpak, S.; Gordon, F.E.; Forsley, L.P.G. (2009) "Triple Tracks in CR-39 as the Result of Pd-D Co-deposition: Evidence of Energetic Neutrons, " *Naturwissenschaften* **96**: 135-142.
[34] Mosier-Boss, P.A.; Dea, J.Y.; Forsley, F.P.G.; Morey, M.S.; Tinsley, J.R.; Hurley, J.P.; Gordon, F.E. (2010) "Comparison of Pd/D Co-deposition and DT Neutron Generated Triple Tracks Observed in CR-39 Detectors," (2010) *Eur. Phys. J. Appl. Phys.* **51**: 20901.
[35] Phillips, G.W.; Spann, J.E.; Bogard, J.S.; VoDinh, T.; Emfietzoglou, D.; Devine, R.T.; Moscovitch, M. (2006) "Neutron Spectrometry Using CR-39 Track Etch Detectors," *Radiat. Prot. Dosim.* **120**: 457-460.
[36] http://www.nnss.gov/docs/docs_FRMAC/_FRMAC_GammaSpec_KnowledgeGuide_2019-08_UUR.pdf
[37] Mosier-Boss, P.A.; Forsley, L.P.; McDaniel, P. (2019) "Uranium Fission Using Pd/D Co-deposition," *Journal of Condensed Nuclear Science* **29**: 219-229. https://www.lenr-canr.org/acrobat/BiberianJPjcondensedzb.pdf#page=228
[38] Petra M.; Swift G.; Landsberger S. (1990) "Design of a Ge NaI(Tl) Compton Suppression Spectrometer and its use in Neutron Activation Analysis," *Nucl. Instr. Meth. A.* **299**: 85-87.
[39] Landsberger S.; Peshev S. (1996) "Compton Suppression Neutron Activation Analysis: Past, Present and Future," *J. Radioanal. Nucl. Chem.* **202**: 201-224.
[40] Nicholson G.; Landsberger S.; Welch L.; Gritzo R. (2008) "Characterization of a Compton Suppression System and the Applicability of Poisson Statistics," *J. Radioanal. Nucl. Chem.* **276**: 577-581.
[41] https://www.amptek.com/internal-products/uranium-and-plutonium-spectra
[42] Decay Chains, http://metadata.berkeley.edu/nuclear-forensics/Decay%20Chains.html
[43] McKubre, M.C.H.; Tanzella, F.L. (1998) "Materials Issues of Loading Deuterium into Palladium and the Association with Excess Heat Production," *in Proceedings of ICCF-7 International Conference on Condensed Matter Nuclear Science*. Vancouver, Canada. https://www.lenr-canr.org/acrobat/McKubreMCHmaterialsi.pdf
[44] McKubre, M.; Tanzella, F.; Hagelstein, P.; Mullican, K.; Trevithick, M. (2003) "The Need for Triggering in Cold Fusion Reactions," *in Proceedings of ICCF-10 International Conference on Condensed Matter Nuclear Science*. Cambridge, MA. https://www.lenr-canr.org/acrobat/McKubreMCHtheneedfor.pdf
[45] Li, X.Z.; Liu, B.; Tian, J.; Wei, Q.M.; Zhou, R,; Yu, Z.W. (2003) "Correlation between Abnormal Deuterium Flux and Heat Flow in a D/Pd System," *J. Phys. D. Appl. Phys.* **36**: 3095-3097. https://www.lenr-canr.org/acrobat/LiXZcorrelatio.pdf
[46] Krishnan, M.; Malhotra, S.; Gaonkar, D.; Srinivasan, M.; Sikka, S.; Shyam, A.; Chitra, V.; Iyengar, T.; Iyengar. P. (1989) "Cold Fusion Experiments using Commercial Pd-Ni Electrolyser," *BARC Studies in Cold Fusion*, P. Iyengar and M. Srinivasab (Eds.) Bhabha Atomic Research Centre, Trombay, Bombay, India, **A1**: 1-10. https://www.lenr-canr.org/acrobat/KrishnanMScoldfusion.pdf
[47] Ilić, R.; Rant, J.; Šutej, T.; Krištof, E.; Skvarè, J.; Koželj, M.; Najžer, M.; Humar, M.; Èerèek, M.; Glumac, B.; Cvikl, B.; Fajgeli, A.; Gyergyek, T.; Trkov, A.; Loose, A.; Peternelj, J.; Remec, I.; Ravnik, M. (1990) "A Search for Neutrons, Protons, Tritons, ^{3}He Ions, Gamma- and X-rays from Deuterium-Deuterium Nuclear Reaction in Electrochemically Charged Palladium," *Nucl. Tracks Radiat. Meas.* **17**: 483-490.
[48] Nagel, D.J. (2013) "Characteristics and Energetics of Craters in LENR Experimental Materials," *J. Condensed Matter Nucl. Sci.* **10**: 1-14. https://www.lenr-canr.org/acrobat/BiberianJPjcondensedi.pdf#page=6
[49] Szpak, S.; Mosier-Boss P.A.; Young, C.; Gordon, F.E. (2005) "Evidence of Nuclear Reactions in the Pd Lattice," *Naturwissenschaften* **92**: 394-393. https://www.lenr-canr.org/acrobat/SzpakSevidenceof.pdf
[50] Srinivasan, M. (1991) "Nuclear Fusion in an Atomic Lattice: An Update on the International Status of Cold Fusion Research," *Curr. Sci.* **60**: 417-439. https://www.lenr-canr.org/acrobat/Srinivasannuclearfus.pdf
[51] De Ninno, A.; Frattolillo, A.; Lollobattista, G.; Martinis, L.; Martone, M.; Mori, L.; Podda, S.; Scaramuzzi, F. (1989) "Evidence of Emission of Neutrons from a Titanium-Deuterium System," *Europhys. Lett.* **9**: 221-224.
[52] Raj, P.; Suryanarayana, P.; Sathyamoorthy, A.; Datta, T. (1989)) "Search for Nuclear Fusion in Gas Phase Deuteriding of Titanium Metal," *BARC Studies in Cold Fusion*, P. Iyengar and M. Srinivasab (Eds.) Bhabha Atomic Research Centre, Trombay, Bombay, India, **B1**: 1-4. https://www.lenr-canr.org/acrobat/RajPsearchforn.pdf

[53] Kamm, G.N.; Ehrlich, A.C.; Gillespie, D.J.; Powers, W.J. (1989) "Search for Neutrons from a Titanium-Deuteride System," *Fusion Technol*. **16**: 401-403.
[54] Miljanić, Š.; Jevtiæ, N.; Pešiæ, S.; Ninkoviæ, M.; Nikoliæ, D.; Josipoviæ, M.; Petrovska, Lj.; Baèiæ, S.; Šutej, T.; Matiæ, S. (1990) "An Attempt to Replicate Cold Fusion Claims" *Fusion Technol*. **18**: 340-346.
[55] Menlove, H.O.; Paciotti, M.A.; Claytor, T.N.; Maltrud, H.R.; Rivera, O.M.; Tuggle, D.G.; Jones, S.E. (1990) "Reproducible Neutron Measurements from Ti Metal in Pressurized D_2 Gas," *in AIP Conference Proceedings on Anomalous Nuclear Effects in Deuterium/Solid Systems*. Provo, UT. https://www.lenr-canr.org/acrobat/MenloveHOreproducib.pdf
[56] Prato, P.; Ricco, G.; Taiti, M.; Boragno, C.; Eggenhoffner, R.; Valbusa, U. (1992) "Search for Neutron Emission from Titanium-Deuterium Systems," *Il Nuovo Cimento* **105A**: 293-299.
[57] Nagel, D.J. (2007) "Powers, Materials and Radiations from Low Energy Nuclear Reactions on Surfaces," *in Proceedings of ICCF-13 International Conference on Condensed Matter Nuclear Science*. Sochi, Russia. https://www.lenr-canr.org/acrobat/NagelDJpowersmate.pdf
[58] Mosier-Boss, P.A.; Forsley, L.P.G.; McDaniel, P.J. (2014) "The Use of CR-39 Detectors in LENR Experiments," *J. Condensed Matter Nucl. Sci*. **14**: 29-49. https://www.lenr-canr.org/acrobat/BiberianJPjcondensedm.pdf#page=35
[59] Cartwright, B.G.; Shirk, W.K.; Price, P.B. (1978) "A Nuclear-Track Recording Polymer of Unique Sensitivity and Resolution," *Nucl. Instrum. Meth*. **153**: 457-460.
[60] Price, P.B.; Barwick, S.W.; Williams, W.T. (1989) "Search for Energetic-Charged-Particle Emission from Deuterated Ti and Pd Foils." *Phys. Rev. Lett*. **63**: 1926-1929.
[61] Li, X.; Dong, S.; Wang, K.; Fang, Y.; Chang, L.; Luo, C.; Hu, R.; Zhou, P.; Mo, D.; Zhu, Y,; Song, C.; Chen, .; Yao, M.; Ren. C.; Chen, Q. (1990) "The Precursor of "Cold Fusion' Phenomenon in Deuterium/Solid Systems." *in AIP Conference Proceedings on Anomalous Nuclear Effects in Deuterium/Solid Systems*. Provo, UT. https://www.lenr-canr.org/acrobat/LiXZtheprecurs.pdf
[62] Li, X.-Z.; Mo, D.-W.; Zhang, L.; Wang, S.-C.; Kang, T.-S.; Liu, S.J.; Wang, J. (1993) "Anomalous Nuclear Phenomena and Solid State Nuclear Track Detector," *Nucl. Tracks Radiat. Meas*. **22**: 599-604.
[63] Jin, S.-X.; Zhang, F.-X.; Liu, Y.-Z. (1993) "Deuterium Absorbability and Anomalous Nuclear Effect of YBCO High Temperature Super-Conductor," *in Proceedings of ICCF-4 International Conference on Condensed Matter Nuclear Science*. Lahaina, Maui.
[64] Jin, S.-X.; Zhang, F.-X.; Liu, Y.-Z.; Shi, W.-Q.; Ou, W.; Liu, S.-X.; Liu, X.-J. (1994) "Deuterium Absorbability and Anomalous Nuclear Effect of YBCO High Temperature Superconductors," *Chin. Sci. Bull*. 39: 101-103.
[65] Ziegler, J.F.; Zabel, T.H.; Cuomo, J.J.; Brusic, V.A.; Cargill III, G.S.; O'Sullivan, E.J.; Marwick, A.D. (1989) "Electrochemical Experiments in Cold Nuclear Fusion," *Phys. Rev. Lett*. **62**: 2929-2932.
[66] http://www.srim.org/
[67] Bockris, J. O'M.; Lin, G.H.; Kainthla, R.C.; Packham, N.J.C.; Velev, O. (1990) "Does Tritium Form at Electrodes by Nuclear Reactions?" *in Proceedings of ICCF-1 International Conference on Condensed Matter Nuclear Science*. Salt Lake City, UT. https://www.lenr-canr.org/acrobat/BockrisJdoestritiu.pdf
[68] Bertulani, C.A. (2009) "Theory and Applications of Coulomb Excitation," https://www.researchgate.net/publication/45869659_Theory_and_Applications_of_Coulomb_Excitation
[69] Glasmacher, T. (1998) "Coulomb Excitation at Intermediate Energies," *Annu. Rev. Nucl. Part. Sci*. **48**: 1-31.
[70] Blewett, M.H. (1967) "Characteristics of Typical Accelerators," *Annu. Rev. Nucl. Part. Sci*. **17**: 427-468.
[71] Bennington, S.M.; Sokhi, R.S.; Stonadge, P.R.; Ross, D.K.; Benham, M.J.; Beynon, T.D.; Whithey, P.; Harris, I.R.; Farr, J.P.G. (1989) "A Search for the Emission of X-rays from Electrolytically Charged Palladium-Deuterium," *Electrochim. Acta* **34**: 1323-1326.
[72] Deakin, M.R.; Fox, J.D.; Kemper, K.W.; Myers, E.G.; Shelton, W.N.; Skofronick, J.G. (1989) "Search for Cold Fusion using X-ray Detection," *Phys. Rev. C* **40**: R1851-R1853.
[73] Mosier-Boss, P.A.; Szpak, S.; Gordon. F.E.; Forsley, L.P.G. (2007) "Use of CR-39 in Pd/D Co-deposition Experiments," *Eur. Phys. J. Appl. Phys*. **40**: 293-303.
[74] Forsley, L.P.; Mosier-Boss, P.A.; McDaniel, P.J.; Gordon, F.E. (2013) "Charged Particle Detection in the Pd/D System: CR-39 SSNTD vs. Real-Time Measurement of Charged Particle Stimulated Pd K Shell X-rays," *Electrochim. Acta* **88**: 373-383.
[75] http://nucleardata.nuclear.lu.se/toi/perchart.htm

[76] Huizenga, J. R. *et al,* Report of the Cold Fusion Panel, Nov. 1989; Published by *US Dept. of Energy*, Washington DC, USA. http://newenergytimes.com/v2/government/DOE1989/19891108-ERAB-Final.pdf
[77] https://www.acs.org/content/acs/en/education/whatischemistry/landmarks/kolthoff-analytical-chemistry.html
[78] Aharoni, A. (1995) "Agreement Between Theory and Experiment," *Physics Today*, **48**: 33-37.
[79] Rothwell, J. (1999) "Transistors and Cold Fusion – Part 1," *Infinite Energy* **5** (25): 32-34. https://www.lenr-canr.org/acrobat/RothwellJtransistor.pdf
[80] Rothwell, J. (1999) "Transistors and Cold Fusion – Part 2," *Infinite Energy* **5** (26): 46-49. https://www.lenr-canr.org/acrobat/RothwellJtransistora.pdf
[81] Bolli, R. (2015) "Reflections on the Irreproducibility of Scientific Papers," *Circ. Res.* **117**: 665-666.
[82] Resnik, D.B., Shamoo, A.E. (2017) "Reproducibility and Research Integity," *Account Res.* **24**: 116-123.
[83] Loscalzo, J. (2012) "Experimental Irreproducibility: Causes, (Mis)interpretations, and Consequences," *Circulation* **125**: 1211-1214.
[84] Lehrer, J. (Dec, 13, 2010) "The Truth Wears Off," *The New Yorker*.
[85] Pines, V; Pines, M.; Chait A.; Steinetz, B. M.; Forsley, L.; Hendricks, R.C.; Fralick, G.C.; Benyo, T. L.; Baramsai, B.; Ugorowski, P.B.; Becks, M. D.; Martin, R.E.; Penney, N.; Sandifer II, C.E., "Nuclear Fusion Reactions in Deuterated Metals", *Physical Review C*, **101** (2020) 044609 and *NASA/TP-20205001617*
[86] Violante, V.; Sarto, F.; McKubre, M.; Tanzella, F.; Hubler, G.; Knies, D.; Grabowski, K.; Zilov, T.; Dardik, I.; Sibilia, C. (2007) "Joint Scientific Advances in Condensed Matter Nuclear Science," *in Proceedings of the* 8^{th} *International Workshop on Anomalies in Hydrogen/Deuterium Loaded Metals*. Sicily, Italy. https://www.lenr-canr.org/acrobat/ViolanteVjointscien.pdf
[87] Violante, V.; Castagna, E.; Lecci, S.; Sansovini, M.; Hubler, G.; Knies, D.; Grabowski, K.; McKubre, M.; Tanzella, F.; Sibilia, C.; Del Prete, Z.; Zilov, T. (2009) "Evolution and Progress in Material Science for Studying the Fleischmann and Pons Effect (FPE)," *in Proceedings of ICCF-15 International Conference on Condensed Matter Nuclear Science*. Rome, Italy. https://www.lenr-canr.org/acrobat/ViolanteVevolutiona.pdf
[88] Violante, V.; Sarto, F.; Castagna, E.; Lecci, S.; Sansovini, M.; McKubre, M.; Tanzella, F. (2012) "The Study of the Fleischmann and Pons Effect through the Materials Science Development," *J. Condensed Matter Nucl. Sci.* **8**: 60-74. https://www.lenr-canr.org/acrobat/BiberianJPjcondensedg.pdf#page=66
[89] Bockris, J. O'M; Sundaresan, R.; Minevski, Z.; Letts, D. (1993) "Triggering of Heat and Sub-Surface Changes in Pd-D Systems," *in Proceedings of ICCF-4 International Conference on Condensed Matter Nuclear Science*. Lahaina, Maui, HI. https://www.lenr-canr.org/acrobat/BockrisJtriggering.pdf
[90] Cravens, D.J.; Letts, D.G. (2003) "Practical Techniques in CF Research – Triggering Methods," *in Proceedings of ICCF-10 International Conference on Condensed Matter Nuclear Science*. Cambridge, MA. https://www.lenr-canr.org/acrobat/CravensDpracticalt.pdf
[91] Mosier-Boss, P.A.; Dea, J.Y.; Gordon, F.E.; Forsley, L.P.G.; Miles, M.H. (2011) "Review of Twenty Years of LENR Research Using Pd/D Co-deposition," *J. Condensed Matter Nucl. Sci.* **4**: 173-187. https://www.lenr-canr.org/acrobat/BiberianJPjcondensedc.pdf#page=181
[92] Violante, V.; Castagna, E.; Sibilia, C.; Paoloni, S.; Sarto, F.; (2003) "Analysis of Ni-Hydride Thin Film after Surface Plasmons Generation by Laser Technique," *in Proceedings of ICCF-10 International Conference on Condensed Matter Nuclear Science*. Cambridge, MA. https://www.lenr-canr.org/acrobat/ViolanteVanalysisof.pdf
[93] Violante, V.; Bertolotti, M.; Castagna, E.; Dardik, I.; McKubre, M.; Moretti, S.; Lesin, S.; Sibilia, C.; Sarto, F.; Tanzella, F.; Zilov, T. (2005) "Progress in Excess Power Production by Laser Triggering," *in Proceedings of ICCF-12 International Conference on Condensed Matter Nuclear Science*. Yokohama, Japan. https://www.lenr-canr.org/acrobat/ViolanteVprogressina.pdf
[94] Mastromatteo, U. (2016) "LENR Anomalies in Pd-H_2 Systems Submitted to Laser Stimulation," *J. Condensed Matter Nucl. Sci.* **19**: 173-182. https://www.lenr-canr.org/acrobat/BiberianJPjcondensedr.pdf#page=181

Appendix

Table of Contents for this Paper

Section/Title	*Page*
Abstract	[1]
1. Introduction	[1]
2. Calorimetry and Helium-4	[2]
2.1. Summary of Fleischmann–Pons Cells and Calorimeter	[2]
2.2. Caltech (U.S.)	[4]
2.3. Harwell (U.K.)	[5]
2.4. MIT (U.S.) and Scientific Misconduct	[5]
2.5. Earthtech (U.S.) and MOAC	[6]
2.6. Helium-4 Measurements	[6]
2.6.1. Naval Air Warfare Center China Lake (U.S.)	[6]
2.6.2. Caltech (U.S.)	[7]
3. Gas Loading	[7]
3.1. SRI (U.S.)	[7]
3.2. Naval Research Laboratory (U.S.)	[8]
4. Neutron Detection	[8]
4.1. Neutron Detection Using NaI, ^{235}U/Lexan Sandwiches, and HPGe	[9]
4.1.1. Salamon Measurements (University of Utah, U.S.)	[9]
4.1.2. Pons and Fleischmann Measurements (University of Utah, U.S.)	[11]
4.1.3. Comparing Salamon and Pons–Fleischmann Results	[12]
4.1.4. Lead Shielding Interactions	[12]
4.2. D Flux in the Metal Lattice	[13]
4.2.1. BARC (India) Experiments	[14]
4.2.2. J. Stefan Institute, E. Kardelj University (Yugoslavia)	[15]
4.3. Detection of Neutron Emissions during Ti/D Gas Loading	[16]
4.3.1. ENEA (Italy)	[16]
4.3.2. Replications	[17]
5. Charged Particle Detection	[17]
5.1. Use of CR-39 to Detect Energetic Charged Particles	[17]
5.1.1. UC Berkeley (U.S.)	[18]
5.1.2. Tsinghua University (China)	[18]
5.1.3. Graduate School, University of Science and Technology of China	[19]
5.2. Use of SSB to Detect Energetic Charged Particles	[20]
5.2.1. IBM (U.S.)	[20]
5.3. X-ray/γ-ray Detection of Energetic Particles	[21]
6. Conclusions	[25]
References	[26]